

HARMONIC FREQUENCY ESTIMATION UNDER NON SINUSOIDAL CONDITIONS

A THESIS

SUBMITTED IN PARTIAL FULFILLMENT OF THE
REQUIREMENTS FOR THE DEGREE OF

MASTER OF TECHNOLOGY

IN

POWER CONTROL AND DRIVES

By

Ms. MONALISA DASH



Department of Electrical Engineering

National institute of Technology

Rourkela-769008

2007

HARMONIC FREQUENCY ESTIMATION UNDER NON SINUSOIDAL CONDITIONS

A THESIS

SUBMITTED IN PARTIAL FULFILLMENT OF THE
REQUIREMENTS FOR THE DEGREE OF

MASTER OF TECHNOLOGY

IN

POWER CONTROL AND DRIVES

By

Ms. MONALISA DASH

Under the Guidance of

Prof. P.C. PANDA

&

Prof. S. ROUTA



Department of Electrical Engineering

National institute of Technology

Rourkela-769008

2007



**National institute of Technology
Rourkela**

CERTIFICATE

This is to certify that the thesis entitled “**Harmonic Frequency Estimation Under Non-Sinusoidal Conditions**” submitted by **Ms. Monalisa Dash**, in partial fulfillment of the requirements for the award of Master of Technology in the Department of Electrical Engineering, with specialization in ‘**Power Control and Drives**’ at National Institute of Technology, Rourkela (Deemed University) is an authentic work carried out by her under my supervision and guidance.

To the best of my knowledge, the matter embodied in the thesis has not been submitted to any other University/Institute for the award of any Degree or Diploma.

Prof. P.C.PANDA
Department of Electrical Engineering
NATIONAL INSTITUTE OF
TECHNOLOGY
Rourkela-769008

Prof. S. Routa
Department of Electrical Engineering
NATIONAL INSTITUTE OF
TECHNOLOGY
Rourkela-769008

DEDICATED TO MY GRAND PARENTS

ACKNOWLEDGEMENTS

On the submission of my thesis report of “**Harmonic Frequency Estimation Under Non-Sinusoidal Conditions**”, I would like to extend my gratitude & my sincere thanks to my supervisors **Prof. P.C.Panda** and **Prof. S.Routa**, Department of Electrical Engineering for their constant motivation and support during the course of my work in the last one year. I truly appreciate and value their esteemed guidance and encouragement from the beginning to the end of this thesis. I am indebted to them for having helped me shape the problem and providing insights towards the solution.

I express my gratitude to Dr.P.K.Nanda, Professor and Head of the Department, Electrical Engineering for his invaluable suggestions and constant encouragement all through the thesis work.

I will be failing in my duty if I do not mention the laboratory staff and administrative staff of this department for their timely help.

I would like to thank all whose direct and indirect support helped me completing my thesis in time.

This thesis would have been impossible if not for the perpetual moral support from my family members, and my friends. I would like to thank them all.

Monalisa Dash

M.Tech (Power Control and Drives)

CONTENTS

ABSTRACT	(iv)
LIST OF FIGURES	(v)
LIST OF TABLES	(vii)
CHAPTER 1	
1.1 INTRODUCTION	1
1.2 OBJECTIVE	2
1.3 REVIEW OF PREVIOUS METHODS	3
1.3.1 ZERO CROSSING METHODS	3
1.3.2 QUADRATIC FORM	3
1.3.3 EIGENVALUE METHOD OF FREQUENCY ESTIMATION	3
1.3.3.1 SIMULATED RESULTS	5
1.3.4 DEMODULATION METHOD	8
1.3.4.1 SIMULATED RESULTS	9
CHAPTER 2	
2.1 NUMERICAL DIFFERENTIATION	15
2.2 DIGITAL FIR FILTER	17
2.3 METHODOLOGY	17
2.3.1 DIGITAL FIR FILTER	18
2.3.2 WINDOWED DIGITAL FIR FILTER	19
2.3.3 SIGNAL DECOMPOSITION	20
2.3.4 FREQUENCY ESTIMATION OF SINUSOIDAL SIGNALS	21

2.3.5	HARMONIC FREQUENCY ESTIMATION	22
2.4	IMPLEMENTATION	22
CHAPTER 3		
3.1	SIMULATION	24
3.2	RESULTS	27
3.3	DISCUSSION	36
CHAPTER 4		
4.1	CONCLUSION	39
4.2	SCOPE OF FUTURE WORK	39
	REFERENCES	40

ABSTRACT

Accurate estimation of power system fundamental frequency is a necessity to check the state of health of the power index. This paper presents a hybrid technique for harmonic frequency estimation of non-sinusoidal signals of power systems with high order harmonics using central numerical differentiation and digital FIR filter algorithm. A digital low-pass FIR filter is used to obtain the discrete values of the fundamental sinusoidal component, and a set of digital band-pass FIR filter is applied to compute the discrete values of the harmonic component. Using 6 points numerical differentiation, these discrete values are used for fundamental and harmonic frequency estimation. For a signal with 5 harmonics, the technique requires at most 2 cycles for the first time of estimation computation, and requires at most 1 cycle for the latter estimation. Comparing with other existing techniques, the proposed algorithm is characteristic of high accuracy and much less time. With satisfactory results, a study example is given to illustrate the proposed algorithm in Matlab.

LIST OF FIGURES

Figure No.	Description	Page No.
Figure 1.1	Model for obtaining two sample sets using Filter	5
Figure 1.2	Complex eigen value estimates for signal with $\omega_1 = 1$ and $\omega_2 = 11$	6
Figure 1.3	Asymptotic bias of estimates	7
Figure 1.4	Error vs. sampling time	7
Figure 1.5	Complex eigen value estimates for signal with $\omega_1 = 314.16$	8
Figure 1.6	Real and imaginary parts of complex input signal V and the demodulation signal Z.	10
Figure 1.7	True frequency and unfiltered estimate for SNR=80dB.	11
Figure 1.8	True and filtered estimate for SNR=80dB.	11
Figure 1.9	True frequency and unfiltered estimate for SNR=40dB.	12
Figure 1.10	True and filtered estimate for SNR=40dB.	12
Figure 1.11	True and estimated frequency for SNR=80dB (time-varying frequency).	13
Figure 1.12	True frequency and unfiltered estimate for SNR=40dB (time-varying frequency).	13
Figure1.13	True and filtered estimate for SNR=40dB (time-varying frequency).	14
Figure 2.1	Numerical differentiation	15
Figure 2.2	Digital FIR Filter	18

Figure 3.2	Sensitivity analysis of frequency estimation of 1 st harmonic for the amplitude of 1 st harmonic.	29
Figure 3.3	Sensitivity analysis of frequency estimation of 1 st harmonic for the phase angle of 1 st harmonic.	29
Figure 3.4	Sensitivity analysis of frequency estimation of 2 nd harmonic for the amplitude of 2 nd harmonic.	30
Figure 3.5	Sensitivity analysis of frequency estimation of 2 nd harmonic for the phase angle of 2 nd harmonic.	30
Figure 3.6	Sensitivity analysis of frequency estimation of 2 nd harmonic with sine noise for the amplitude of 2 nd harmonic.	31
Figure 3.7	Sensitivity analysis of frequency estimation of 3 rd harmonic for the amplitude of 3 rd harmonic.	31
Figure 3.8	Sensitivity analysis of frequency estimation of 3 rd harmonic for the phase angle of 3 rd harmonic.	32
Figure 3.9	Sensitivity analysis of frequency estimation of 4 th harmonic for the amplitude of 4 th harmonic.	32
Figure 3.10	Sensitivity analysis of frequency estimation of 4 th harmonic for the phase angle of 4 th harmonic.	33
Figure 3.11	Sensitivity analysis of frequency estimation of 5 th harmonic for the amplitude of 5 th harmonic.	33
Figure 3.12	Sensitivity analysis of frequency estimation of 5 th harmonic for the phase angle of 5 th harmonic.	34
Figure 3.13	Sensitivity analysis of frequency estimation of 5 th harmonic with sine noise for the amplitude of 5 th harmonic.	34
Figure 3.14	Sensitivity analysis of frequency estimation of 1 st harmonic with noise and time-varying frequency for the amplitude of 5 th harmonic.	35
Figure 3.15	Sensitivity analysis of frequency estimation of 1 st harmonic for the frequency of sine noise.	35

LIST OF TABLES

Table No.	Description	Page No.
Table-I	Frequency estimation of 1 st harmonic of non-sinusoidal signals.	
Table-II	Frequency estimation of 2nd harmonic of non-sinusoidal signals	
Table-III	Frequency estimation of 3rd harmonic of non-sinusoidal signals	
Table-IV	Frequency estimation of 4 th harmonic of non-sinusoidal signals	
Table-V	Frequency estimation of 5 th harmonic of non-sinusoidal signals	
Table-VI	Comparison of techniques	

CHAPTER 1

INTRODUCTION

1.1 INTRODUCTION

Frequency is regarded as an important index of the operation of power systems. By observing frequency variations, utilities can know the system energy balance situations. In steady-state, the system frequency is always kept around 60Hz (or 50Hz). However, frequency may vary away from 60Hz in the transient events. In addition, there are many devices, such as power electronic equipments and arc furnaces, etc. generating lots of harmonics and noise in modern power systems. Frequency shows the dynamic energy balance between load and generating power, phasor can constitute the state of the system, and damping of frequency variation reveals the stability of power system. These parameters can even be used to predict many power systems accidents. So these parameters are regarded as important indices for operating power systems in practice. Besides, these parameters are also useful for protection relays and fault location techniques.

Frequency estimation has been one of the important tasks in measurement, control, relaying protection, distribution automation, and intelligent instrumentation of power system, such as power metering. Accurate power fundamental frequency is a necessity to check the state of health of the power index, and a guarantee for accurate quantitative measurement of power parameters, such as voltages, currents, active power, and energy, reactive power, and energy, and so on, in multifunction power meters under steady states.

It is essential for a method that can measure frequency in the presence of harmonics and noise. Therefore, an effective method for frequency estimation is required in both steady-state and in transient-state.

The use of fast and high-performance microprocessors and the development of digital algorithms, such as zero crossing technique [1], Quadratic form based technique [2], least squares error technique [3]–[4], Newton method [5], Kalman filter [6]–[12], Fourier transform [13]–[17], demodulation technique [18], eigenvalue analysis [19] for power frequency estimation bring in more benefits in the fields of measurement, instrumentation, control, and monitor of power systems. List of different techniques are as follows:

- Least mean squares error techniques.
- NLMS technique.
- Adaptive combine filtering technique.
- Kalman filtering.
- Finite impulse response filtering.
- Zero crossing technique.

- Level crossing technique.
- FFT techniques.
- DFT techniques.
- Newton method.
- Prony method
- SDFT technique, etc

The typical use of frequency estimation in power systems is for protection scheme against loss of synchronism, under-frequency relaying and for power system stabilization. The applications can be categorized based on their time demand, that is,

- critical real time applications, such as relay protection;
- on-line data monitoring in control room;
- Off-line data analysis of computer recordings.

The classification is useful since the different time demands put restrictions on what type of frequency estimator and filter technique that can be used. In off-line data analysis we have access to the full time series and the estimation and filtering can be improved by using noncausal forward-backward filtering. To compare different methods we need a test criterion that reflects relevant demands. Three such demands are:

- speed of convergence;
- accuracy of the estimator; and
- noise rejection.

The key problem is to find a method that improves all these demands and not just compromise one demand for another.

1.2 OBJECTIVE

In the past, many digital algorithms have been proposed to apply to frequency estimation [1-3]. Discrete Fourier Transform (DFT) is the most popular algorithm and widely used in digital relays. However, the accuracy of DFT is affected by frequency deviation. This drawback makes DFT not suitable for frequency estimation in transient-state. A new method of harmonic analysis is discussed here. The proposed technique employs low-pass and band-pass FIR filters to decompose the non-sinusoidal signal into individual sinusoidal components, and then estimate the frequency of each individual sinusoidal components using central numerical differentiation with 6 points. Using 6 points numerical differentiation, these discrete values are used for fundamental and harmonic frequency estimation. For a signal with 5 harmonics, the technique

requires at most 2 cycles for the first time of estimation computation, and requires at most 1 cycle for the latter estimation. Comparing with other existing techniques, the proposed algorithm is characteristic of high accuracy and much less time. With satisfactory results, a study example is given to illustrate the proposed algorithm in Matlab.

1.3 REVIEW OF PREVIOUS WORK

Various frequency tracking methods were studied and its simulation results obtained during the course of study. These have been listed hereof.

1.3.1 Zero Crossing Methods

This is a popular method in both protection and control. When using zero crossing methods, one determines the time between zero crossings of the signal to determine the frequency. This can be carried out by having a sliding window of samples and curve fitting using a least squares technique [2]. This method can be applied to a single phase, but three phases may be used together to provide the frequency at more intervals.

1.3.2 Quadratic Form

This method is described in detail in Hacaoglu [3]. Suppose that we are analyzing a set of signal samples defined by the vector $x = (x[n], x[n-1], \dots, x[n-M+1])$. The quadratic form of x is defined as

$$F(x) = \sum_{m=0}^{M-1} \sum_{k=0}^{M-1} h[k, m] x[n-k] x[n-m]$$

Where $h[k, m]$ is the (k, m) th term of an $(M \times M)$ matrix. A nominal frequency of 50 Hz is assumed. By taking the ratio of two quadratic forms of x with different matrices H_1 and H_2 that it is possible to obtain an approximate formula for the frequency.

1.3.3 Eigenvalue method of Frequency Estimation

Estimating the frequencies of a number of sinusoids in a signal is considered. It is shown that by passing the signal $x(t)$ through a continuous-time filter $f(s)$ to obtain the filtered signal $x_f(t)$, we can obtain the required frequencies from the eigenvalues of the matrix product XX_f^{-1} , where X and X_f are formed from samples of x and x_f respectively. There are two positive points for using a continuous filter instead of a differentiator/integrator ;(1)-relaxing the practical concerns of designing the differentiator/integrator, and (2)-having some freedom in designing the filter so that attenuation of the noise in the signal is possible especially if the noise spectrum is outside the band of frequencies of interest. Utilizing the filtered signal samples relaxes the condition on the lower allowed sampling rate known as Nyquist rate.

The sinusoid amplitude, frequency and phase are A , ω and ϕ respectively. To obtain estimates of the frequencies $\omega_1, \dots, \omega_n$ from measurements of x available at discrete sampling instants kT_s , $k=1, 2, \dots$, the sampling frequency $\omega_s=2\pi/T_s$, must be at least twice the highest frequency in x in order to be able to recover all the frequency components in x . In fact, all sinusoids with frequencies $\omega_i + l\omega_s$, where l is an integer, are indistinguishable if sampled at frequency ω_s because $\sin(\omega_i kT_s + \phi_i) = \sin((\omega_i + l\omega_s)kT_s + \phi_i)$. Variations of the signal in between sampling instants are missed, and this is why it is not possible to distinguish between frequency *aliases*. If the signal is passed through a continuous filter and the filtered signal is sampled at the same frequency as the original signal, we get a new set of samples $x_f(kT)$, which carries some information about the way the original signal is changing in between the sampling instants.

First, assume that the measured signal x is the sum of n sinusoids representing a fundamental plus some harmonics and probably some non-integral harmonics

$$x(t) = \sum_{i=1}^n C_i \sin(\omega_i t + \phi_i) \quad \dots\dots\dots (1.1)$$

Where C_i , ω , ϕ and are the sinusoid's amplitude, frequency, and phase, respectively. Our problem is to obtain estimates of the frequencies such that the required fundamental frequency is among these estimates. The signal in (3) can be written in terms of imaginary exponentials as

$$x(t) = \sum_{i=1}^{2n} A_i e^{\alpha_i t} \quad \dots\dots\dots (1.2)$$

where $\alpha_1, \dots, \alpha_{2n}$ occur in imaginary conjugates $(j\omega_i, -j\omega_i)$, $i=1, \dots, n$ and A_1, \dots, A_{2n} occur in complex conjugates (A_i, A_i^*) . The Laplace transform of the signal is

$$x(s) = \sum_{i=1}^{2n} \frac{A_i}{s - \alpha_i} \quad \dots\dots\dots (1.3)$$

The first step in the proposed method is to obtain a filtered signal x_f by passing x through a continuous filter with rational transfer function in the domain as in Fig.1.1. Samples of x and x_f are taken at the same time instants so that we get two sets of samples. Assuming the order of the filter (i.e., the number of its poles) is m , and then we can write $h(s)$ as

$$h(s) = \sum_{j=1}^m \frac{B_j}{s - \beta_j} \quad \dots\dots\dots (1.4)$$

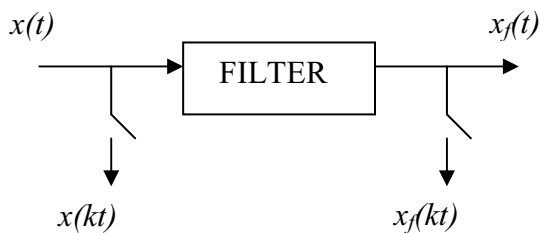


Figure 1.1

Let $X(t)$ be the matrix of signal samples:

$$X(t) = \begin{bmatrix} x(t + \tau_1 + T_1) & x(t + \tau_1 + T_2) & x(t + \tau_1 + T_3) & \dots & x(t + \tau_1 + T_N) \\ x(t + \tau_2 + T_1) & x(t + \tau_2 + T_2) & x(t + \tau_2 + T_3) & \dots & x(t + \tau_2 + T_N) \\ x(t + \tau_3 + T_1) & x(t + \tau_3 + T_2) & x(t + \tau_3 + T_3) & \dots & x(t + \tau_3 + T_N) \\ \vdots & \vdots & \vdots & \ddots & \vdots \\ x(t + \tau_M + T_1) & x(t + \tau_M + T_2) & x(t + \tau_M + T_3) & \dots & x(t + \tau_M + T_N) \end{bmatrix} \dots\dots\dots (1.5)$$

Let $t + \tau_i$ and $i = 1, \dots, M$ be the starting instant of a frame of N samples, and T_j and $j = 1 \dots N$ be the time shifts of individual samples within the frame, measured from the starting of the frame.

$$X(t) = \begin{bmatrix} U_\alpha & U_\beta \end{bmatrix} \begin{bmatrix} \Lambda_\alpha(t) & 0 \\ 0 & 0 \end{bmatrix} \begin{bmatrix} V'_\alpha \\ V'_\beta \end{bmatrix} \dots\dots\dots (1.6)$$

$$X_f(t) = \begin{bmatrix} U_\alpha & U_\beta \end{bmatrix} \begin{bmatrix} \Lambda_\alpha(t)F & 0 \\ 0 & \Lambda_\beta(t)\chi \end{bmatrix} \begin{bmatrix} V'_\alpha \\ V'_\beta \end{bmatrix}$$

Therefore, for square $X(t)$ and $X_f(t)$ with $M=N=2n+m$, and with distinct signal frequencies and filter poles:

$$X_f^{-1}(t)X(t) = \begin{bmatrix} V'_\alpha & V'_\beta \end{bmatrix}^{-1} \begin{bmatrix} F^{-1} & 0 \\ 0 & 0 \end{bmatrix} \begin{bmatrix} V'_\alpha & V'_\beta \end{bmatrix} \dots\dots\dots (1.7)$$

Let $\lambda_1 \dots \lambda_{2n}$ be the nonzero eigenvalues obtained for the pair $[X(t) X_f(t)]$, then because they are equal to the diagonal elements of F^{-1} , it follows that:

$$\lambda_i = \frac{1}{h(\alpha_i)} \dots\dots\dots (1.8)$$

1.3.3.1 RESULTS:

Figure 1(a) shows the estimated eigenvalues $\alpha_1 \dots \alpha_4$ plotted as dots, and the true values $\pm j\omega_1$ and $\pm j\omega_2$, as small circles. The plot shows that the estimated values are clustered around the true values, and that the error is in proportion with the true value (the estimates of the lower frequency seem closer to their true value than the estimates of the higher frequency). The true

values are pure imaginary, but unfortunately the estimates have small real values which are a result of using noisy data. To study the asymptotic statistical behavior of the estimates, fifty runs were taken. The estimation error vector of run number k is defined as $e_k = \alpha - \hat{\alpha}_k$. The mean value of the estimation error up to run k is defined as $m_k = \frac{1}{k} \sum_{i=1}^k e_i$ which approximates the asymptotic bias in the estimate. As can be seen from Figure 1.3, the asymptotic bias in the estimates approaches zeros giving unbiased estimates.

Simulation Results:

1. A test signal of the following form was taken:

$$x(t) = \cos(\omega_1 t) + \cos(\omega_2 t) \quad \dots\dots\dots (1.9)$$

where $\omega_1 = 1$ and $\omega_2 = 11$. Fig 1.2 shows the true and the estimated values.

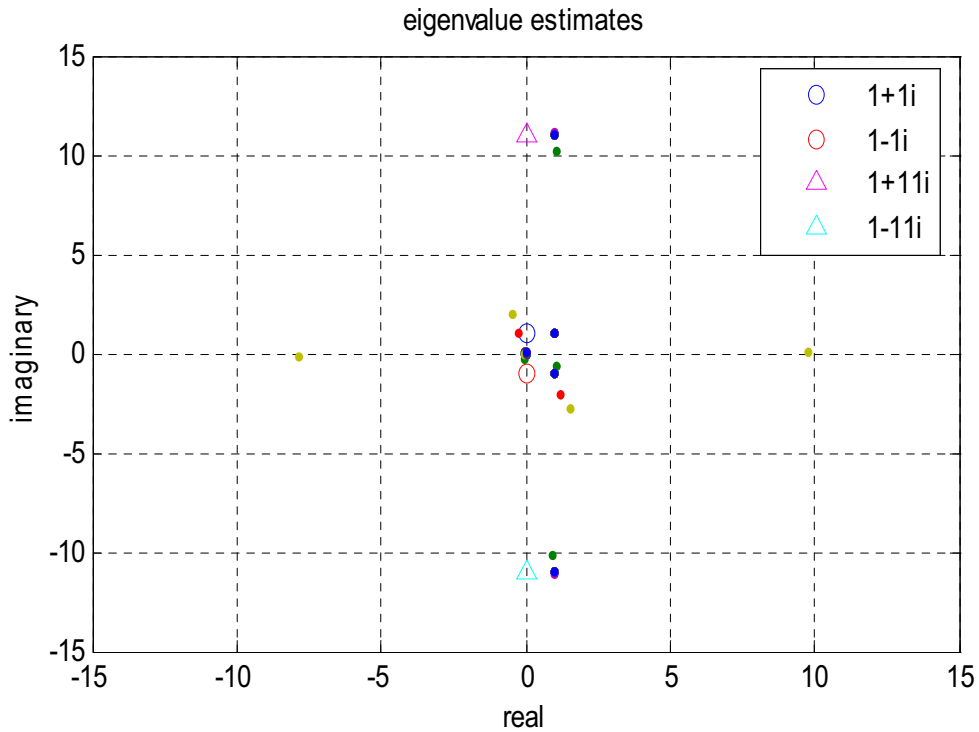


Figure 1.2

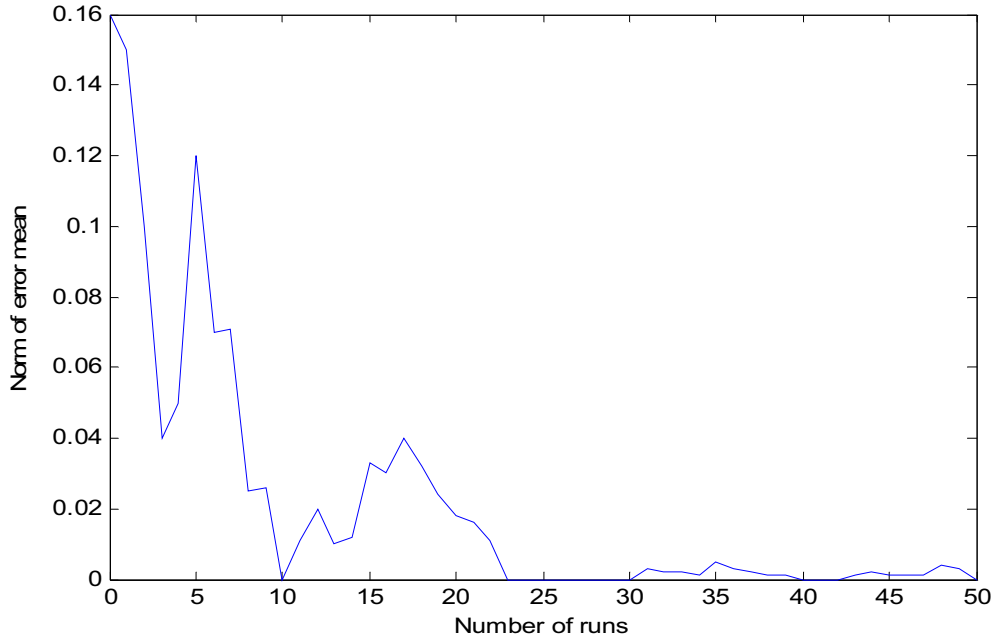


Figure 1.3

On computer simulation it was seen that choice of sampling time plays an important role in giving an accurate estimate. By taking different sampling instants we run the program and plot a graph of the error estimates. It was found that there were a few spikes (as shown in fig.1.4) at certain points indicating points of low accuracy. These are the choice of sampling time T which should be carefully avoided in order to get a more accurate estimate.

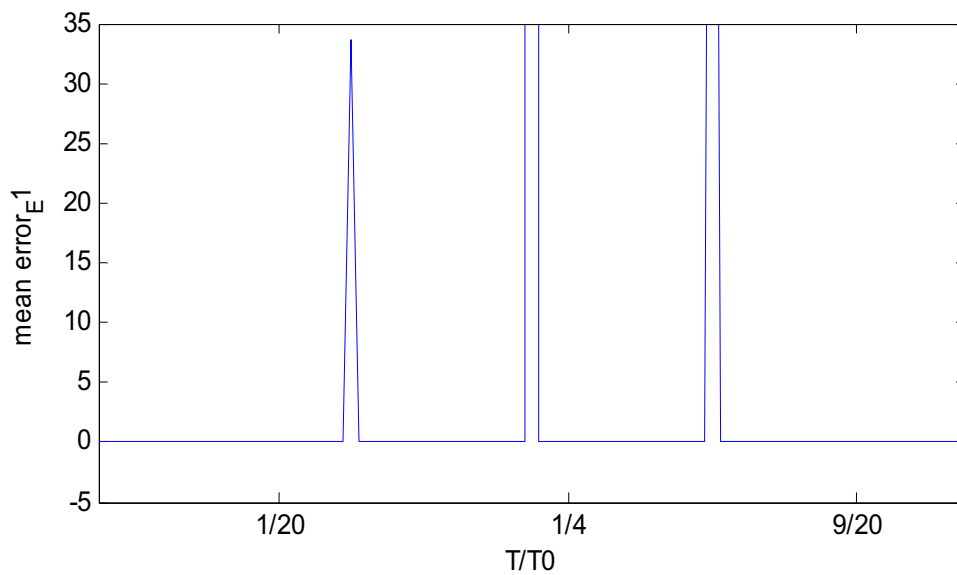


Figure 1.4

2. Another test signal with a frequency of 50 Hz was taken, so that $\pm j\omega_1 = \pm j314.16$. The plot is as shown in figure 1.5.

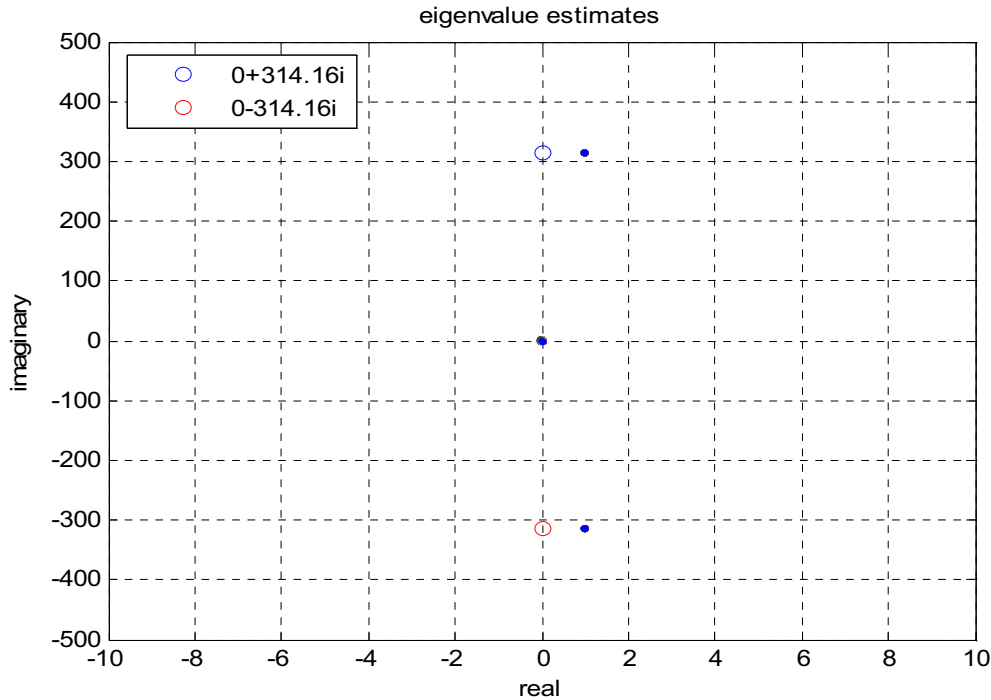


Figure 1.5

1.3.4 Demodulation Method

Consider $v_1(k), v_2(k), v_3(k)$, to be samples of the three phase voltages

$$v_i(k) = \hat{A}_i \sin(\omega_1 t_k) + e_i(k) \quad i = 1, 2, 3 \quad \dots\dots\dots (1.10)$$

where e_i is a general noise term that can be any combination of white noise and harmonics.

The $\alpha\beta$ -components are defined as the complex voltage

$$V(k) = V_\alpha(k) + jV_\beta(k) \quad \dots\dots\dots (1.11)$$

where the real and imaginary parts are calculated from

$$\begin{pmatrix} V_\alpha(k) \\ V_\beta(k) \end{pmatrix} = \sqrt{\frac{2}{3}} \begin{pmatrix} 1 & -1/2 & -1/2 \\ 0 & \sqrt{3}/2 & \sqrt{3}/2 \end{pmatrix} \begin{pmatrix} V_1(k) \\ V_2(k) \\ V_3(k) \end{pmatrix} \quad \dots\dots\dots (1.12)$$

In the literature, the complete transformation is often called the $\alpha\beta 0$ -transform and then also includes the zero sequence component. In our application we only use the two perpendicular parts, α and β , and therefore leave out the zero sequence component in our transformation. Note that V_α , and V_β can contain plus and minus sequence voltage, but not any zero sequence

component. Hence, harmonics that are mainly zero sequence-such as the third harmonic-are blocked by the $\alpha\beta$ transformation.

The input signal without any negative sequence component and noise is given by

$$\begin{aligned} V(k) &= A[\cos(\omega_1 t_k + \phi) + j \sin(\omega_1 t_k + \phi)] \\ &= A e^{j(\omega_1 t_k + \phi)} \end{aligned} \quad \dots\dots\dots (1.13)$$

where A is the phase to phase RMS-value.

The demodulation is done with a complex signal Z that rotates in the opposite direction, i.e., negative sequence, compared to the input signal V.

The signal Z with a known frequency is

$$Z(k) = \cos(-\omega_0 t_k) + j \sin(-\omega_0 t_k) = e^{-j\omega_0 t_k} \quad \dots\dots\dots (1.14)$$

The resulting signal, Y, after the multiplication becomes

$$Y(k) = V(k). Z(k) = A e^{j[(\omega_1 - \omega_0)t_k + \phi]} \quad \dots\dots\dots(1.15)$$

We define the complex variable U as

$$U(k) = Y(k).Y(k-1)^* \quad \dots\dots\dots (1.16)$$

So that the phase difference between two consecutive samples is calculated as

$$\gamma(k) - \gamma(k-1) \approx \arctan\left(\frac{\text{Im}[U(k)]}{\text{Re}[U(k)]}\right) \quad \dots\dots\dots (1.17)$$

The deviation in angular frequency is found to be

$$\Delta\omega(k) = \frac{1}{\Delta t} [\gamma(k) - \gamma(k-1)] = f_s [\gamma(k) - \gamma(k-1)] \quad \dots\dots\dots (1.18)$$

The unknown frequency for the signal V is

$$\hat{f}(k) = f_0 + \frac{f_s}{2\pi} \arctan\left(\frac{\text{Im}[U(k)]}{\text{Re}[U(k)]}\right) \quad \dots\dots\dots (1.19)$$

Where f_0 is the nominal, and f_s , is the sampling frequency.

1.3.4.1 RESULTS:

The real and imaginary parts of input signal V and the demodulation signal Z are plotted overleaf in figure 1.6.

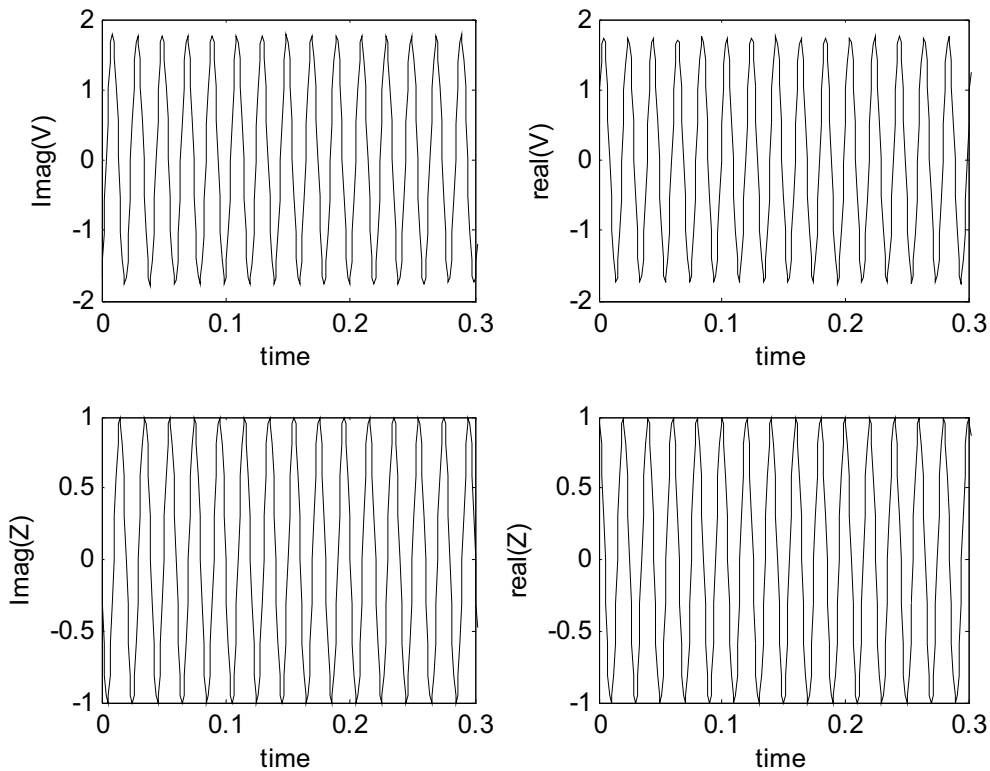


Figure 1.6

1. A test signal was taken where the three phase voltages (without harmonics) are of the form

$$v_i(k) = \sqrt{2} A_{rms} \sin(\phi(k)) + N_i(m, \sigma) \quad i=1, 2, 3 \quad \dots\dots\dots (1.20)$$

Where $\phi_1(0) = 0$; $\phi_2(0) = -\frac{2\pi}{3}$; $\phi_3(0) = \frac{2\pi}{3}$;

The notation $N(m, \sigma)$ is used for normally distributed white noise. A few examples have been taken for different SNR values and the frequency estimation is done for both filtered as well as unfiltered signals.

a) **SNR=80dB**. Standard deviation is $\sigma=0.0001$ and the mean $m=0$. The signal used has an RMS-value of 1 p.u. giving a signal to noise ratio of

$$SNR = 20 \log\left(\frac{1}{0.0001}\right) = 80dB . \quad \dots\dots\dots (1.21)$$

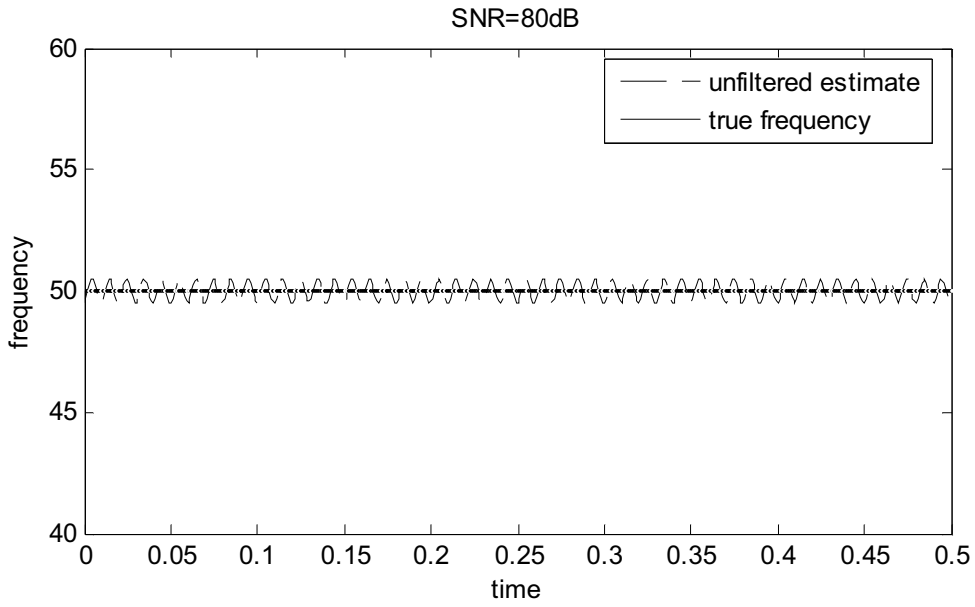


Figure 1.7

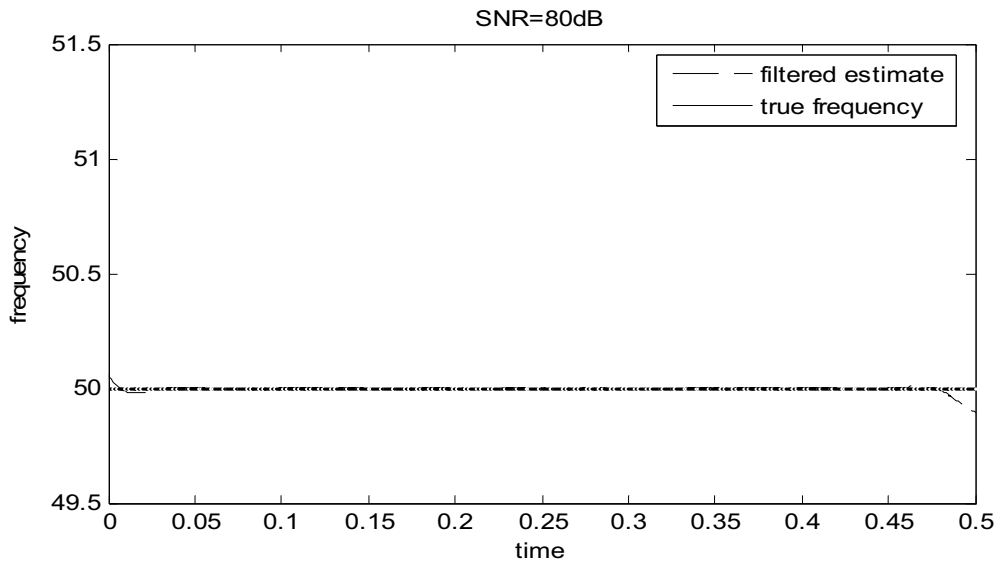


Figure 1.8

b) **SNR=40dB**. Standard deviation is $\sigma=0.01$ and the mean $m=0$. The signal used has an RMS-value of 1 p.u. giving a signal to noise ratio of

$$SNR = 20 \log\left(\frac{1}{0.01}\right) = 40dB$$

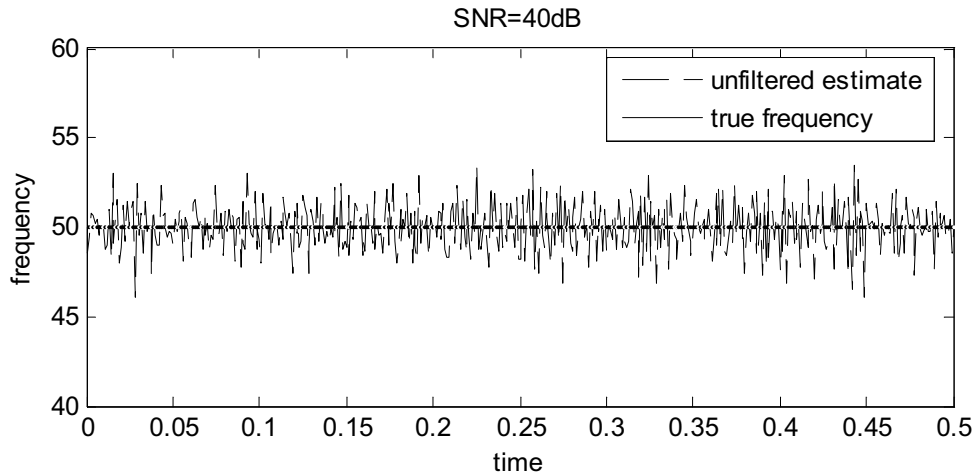


Figure 1.9

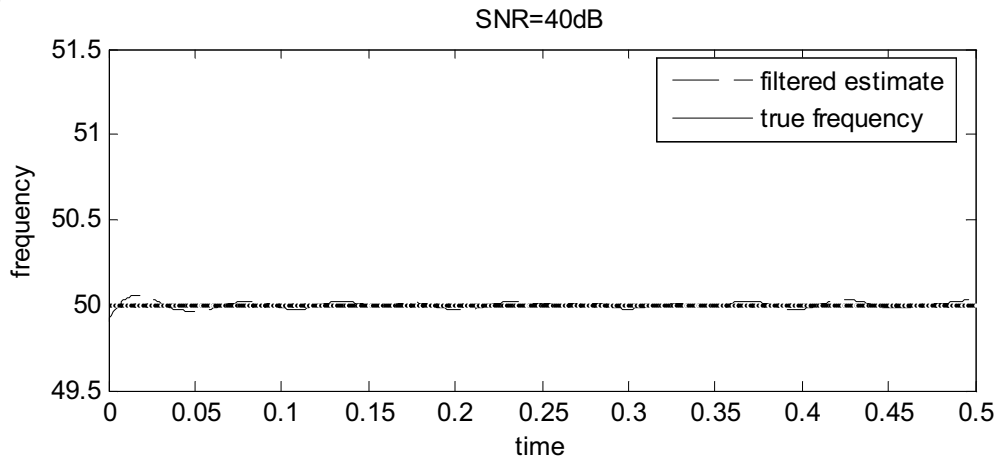


Figure 1.10

2. Test signal of three phase voltages (with harmonics) are taken

$$v_i(k) = \sqrt{2}A_{rms} \sin(\phi(k)) + N_i(m, \sigma) \quad i=1, 2, 3 \quad \dots\dots\dots (1.22)$$

The angles are calculated from

$$\phi_i(k) = \phi_i(k-1) + \omega(k)\Delta t; \quad \text{For } k \geq 1$$

Where $\phi_1(0) = 0$; $\phi_2(0) = -\frac{2\pi}{3}$; $\phi_3(0) = \frac{2\pi}{3}$;

The frequency is time-varying,

$$\omega(k) = 2\pi[50 + \sin(2\pi \cdot 1 \cdot t_k) + 0.5 \sin(2\pi \cdot 6 \cdot t_k)] \dots\dots\dots (1.23)$$

a) **SNR=80dB**

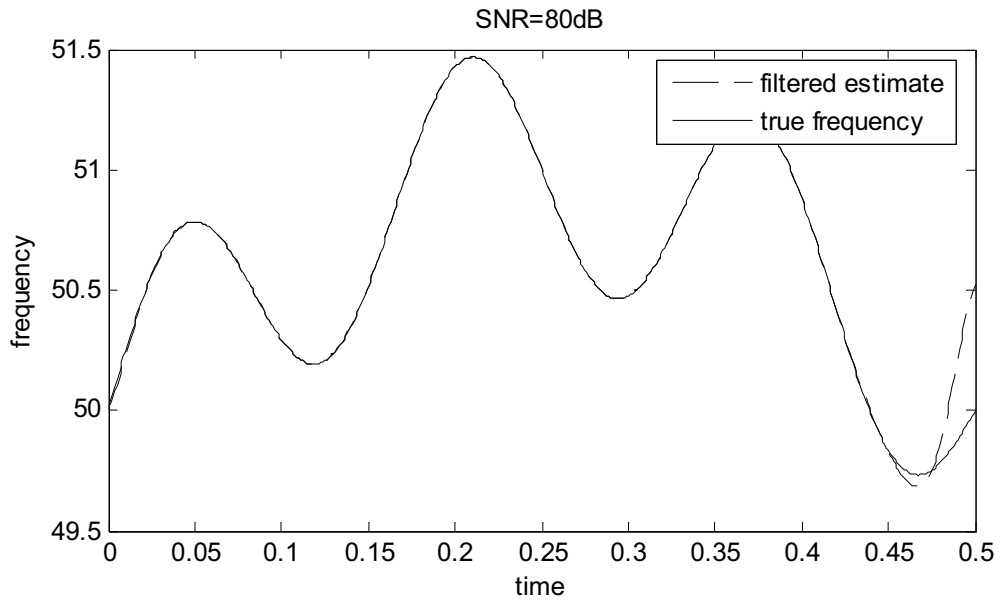


Figure 1.11

b) **SNR=40dB**

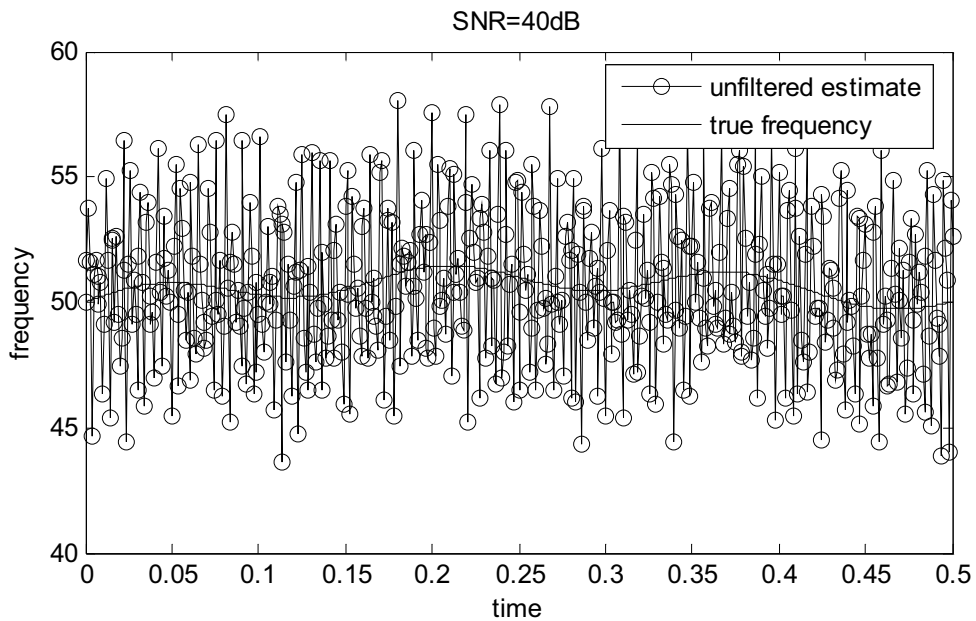


Figure 1.12

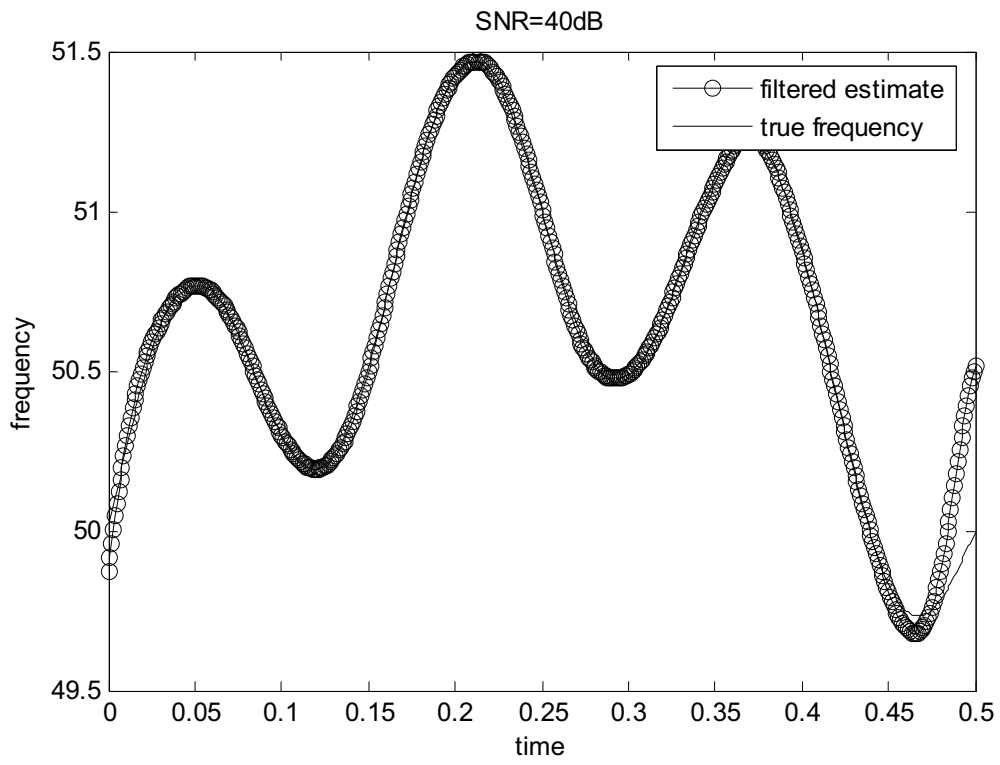


Figure 1.13

CHAPTER 2

HARMONIC FREQUENCY ESTIMATION

2.1 NUMERICAL DIFFERENTIATION

Numerical differentiation is a technique of numerical analysis to produce an estimate of the derivative of a mathematical function or function subroutine using values from the function and perhaps other knowledge about the function.

A simple two-point estimation is to compute the slope of a nearby secant line through the points $(x, f(x))$ and $(x+h, f(x+h))$. Choosing a small number h , h represents a small change in x , and it can be either positive or negative. The slope of this line is as shown in fig. below.

$$\frac{f(x+h) - f(x)}{h} \dots\dots\dots (2.1)$$

This expression is Newton's difference quotient.

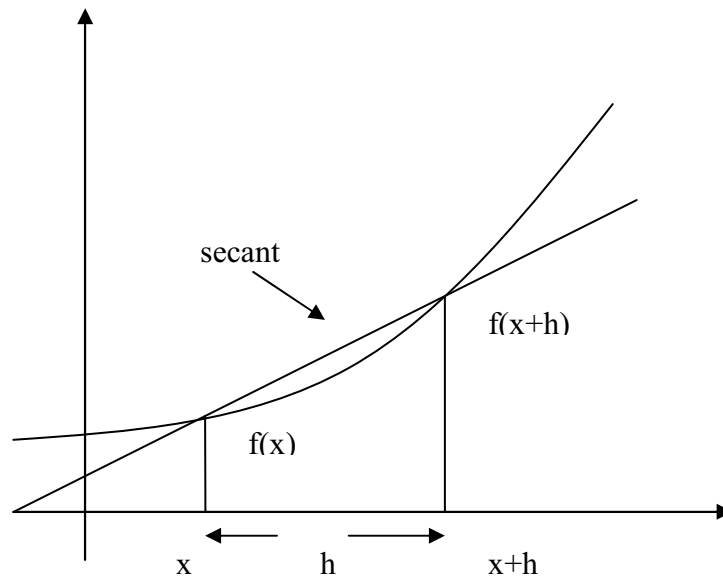


Figure2.1

The slope of this secant line differs from the slope of the tangent line by an amount proportional to h . As h approaches zero, the slope of the secant line approaches the slope of the tangent line. Therefore, the true derivative of f at x is the limit of the value of the difference quotient as the secant lines get closer and closer to being a tangent line:

$$f'(x) = \lim_{h \rightarrow 0} \frac{f(x+h) - f(x)}{h} \dots\dots\dots (2.2)$$

Let $v(t)$ be a function of voltage signal which takes on the values $v(t_i)=0$. At discrete points such as (t_i, v_i) and (t_j, v_j) , $i=0, 1, 2, \dots, M-1, j=0, 1, 2, \dots, M-1$, the Taylor series expansion is expressed as

$$v(t_i) = v(t_j) + \Delta t \left. \frac{dv}{dt} \right|_{t=t_j} + \frac{(\Delta t)^2}{2!} \left. \frac{d^2v}{dt^2} \right|_{t=t_j} + \frac{(\Delta t)^3}{3!} \left. \frac{d^3v}{dt^3} \right|_{t=t_j} + \dots + \frac{(\Delta t)^M}{M!} \left. \frac{d^M v}{dt^M} \right|_{t=t_j} + \dots, \quad \dots\dots\dots (2.3)$$

where $\Delta t=t_i-t_j$.

Without consideration of M order and higher order derivatives, we have central difference formulas such that

$$v(t_{i+j}) = v(t_i) + (t_{i+j} - t_i)v'(t_i) + \frac{(t_{i+j} - t_i)^2}{2!} v''(t_i) + \frac{(t_{i+j} - t_i)^3}{3!} v^{(3)}(t_i) + \dots + \frac{(t_{i+j} - t_i)^{(M-1)}}{(M-1)!} v^{(M-1)}(t_i), \quad \dots\dots\dots (2.4)$$

Where $j=\pm 1, \pm 2, \pm 3, \pm k$. $k=\text{floor}(M/2)$, floor (A) rounds the elements of A to the nearest integers less than or equal to A .

Given $(t_0, v_0), (t_1, v_1), \dots, (t_M, v_M)$ with regular spaced h , we have the following relationship:

$$t_0, t_1 = t_0 + h, t_2 = t_0 + 2h, t_3 = t_0 + 3h, \dots, t_M = t_0 + Mh. \quad \dots\dots\dots(2.5)$$

For $j=1, 2, 3, \dots, k$, Eq. (4) can be expressed as the following formula:

$$v(t_{i+j}) = v(t_i) + khv'(t_i) + \frac{(kh)^2}{2!} v''(t_i) + \frac{(kh)^3}{3!} v^{(3)}(t_i) + \dots + \frac{(kh)^{(M-1)}}{(M-1)!} v^{(M-1)}(t_i), \quad \dots\dots\dots (2.6)$$

For $j=-1, -2, -3, \dots, -k$, Eq. (4) can be expressed as the following formula:

$$v(t_{i-j}) = v(t_i) - khv'(t_i) + \frac{(-kh)^2}{2!} v''(t_i) + \frac{(-kh)^3}{3!} v^{(3)}(t_i) + \dots + \frac{(-kh)^{(M-1)}}{(M-1)!} v^{(M-1)}(t_i), \quad \dots\dots\dots (2.7)$$

With $v(t_{i-k})-v(t_{i+k})$ known, the solution of first and $M-1$ order derivatives are obtained with the help of the above equation set.

For example, with $M=7$, the second order derivative of $v(p)$ at point p is expressed as follows:

$$v''(p) = \{2[v(p+3) + v(p-3)] - 27[v(p+2) + v(p-2)] + 270[v(p+1) + v(p-1)] - 490v(p)\} / 180h^2 \dots\dots\dots (2.8)$$

Also for $M=7$, the fourth order derivative is expressed as:

$$v''''(p) = \{-2[v(p+3) + v(p-3)] + 24[v(p+2) + v(p-2)] - 78[v(p+1) + v(p-1)] + 112v(p)\} / 12h^4 \dots\dots\dots (2.9)$$

2.2 DIGITAL FIR FILTER

Filters are signal conditioners. Each functions by accepting an input signal, blocking prespecified frequency components, and passing the original signal minus those components to the output. There are many filter types, but the most common are low pass, high pass, band pass, and band stop. A low pass filter allows only low frequency signals (below some specified cutoff) through to its output, so it can be used to eliminate high frequencies. A highpass filter does just the opposite, by rejecting only frequency components below some threshold. A band stop filter (as is used in the algorithm) is an electric filter which transmits more or less uniformly at all frequencies of interest except for a band within which frequency components are largely attenuated. Also, it is known as band-elimination filter; band-rejection filter. A tuned circuit designed to stop frequencies between a lower cut-off frequency (f_1) and a higher cut-off frequency (f_2) of the amplifier while passing all other frequencies.

FIR, Finite Impulse Response, filters are one of the primary types of filters used in Digital Signal Processing. FIR filters are said to be finite because they do not have any feedback. Therefore, if you send an impulse through the system (a single spike) then the output will invariably become zero as soon as the impulse runs through the filter.

2.3 METHODOLOGY

This chapter presents a hybrid technique for harmonic frequency estimation of non-sinusoidal signals of power systems with high order harmonics using central numerical differentiation and digital FIR filter algorithm. A novel algorithm proposed in this paper is developed to estimate the fundamental frequency estimation of non-sinusoidal signals with white Gaussian noises using numerical differentiation and central Lagrange interpolation with multi-points. The proposed algorithm can arrive at an accuracy of 0.001% of estimation over a larger range and only spend

at most 1 cycle. Comparing with other algorithms, this algorithm spends little time and computation over a wide range at a high accuracy, so that this proposed algorithm is adaptive to be applied in real-time, intelligent measurement and control cases.

A digital low-pass FIR filter is used to obtain the discrete values of the fundamental sinusoidal component, and a set of digital band-pass FIR filter is applied to compute the discrete values of the harmonic component. Using 6 points numerical differentiation, these discrete values are used for fundamental and harmonic frequency estimation. Comparing with other existing techniques, the proposed algorithm is characteristic of high accuracy and much less time. With satisfactory results, a study example is given to illustrate the proposed algorithm in Matlab.

The proposed technique employs low-pass and band-pass FIR filters to decompose the non-sinusoidal signal into individual sinusoidal components, and then estimate the frequency of each individual sinusoidal components using central numerical differentiation with 6 points. It needs at most 2 cycles for harmonic frequency estimation, so that it can be applied to real-time application cases.

2.3.1 Digital FIR Filter

Filtering is a process of selecting certain frequency components of a multiple-harmonic signal. FIR filters are often used because they are simple and easy to implement. Using dot product, the output of FIR filter is sum of the results of dot product of filter coefficients and the most recent n data samples, as shown in Fig.1.

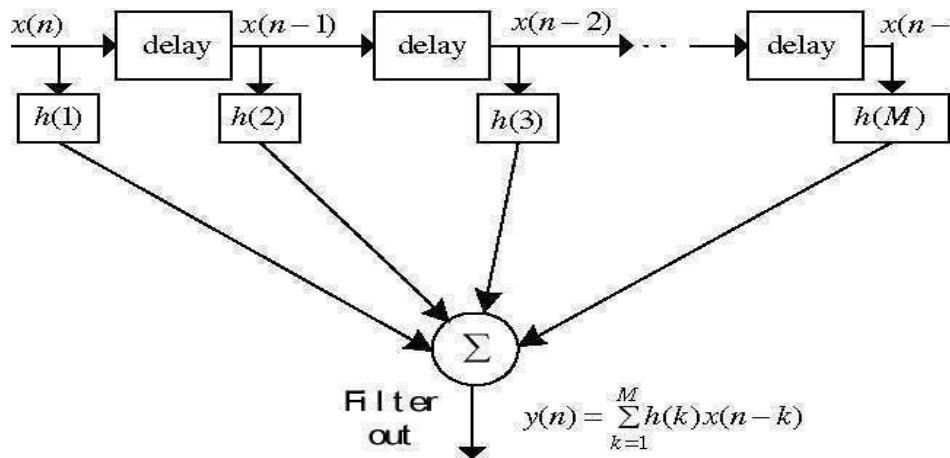


Figure2.2

Let $h(1), h(2), \dots, h(M)$ be the coefficients of a finite impulse response (FIR) filter of length M .

Using input signal $x(n)$, the filter output signal $y(n)$ is defined by the following equation:

$$y(n) = \sum_{k=1}^M h(k)x(n-k) \quad \dots\dots\dots(2.10)$$

The function of the frequency response is defined by:

$$H(e^{j\omega}) = H(\omega)e^{j\theta(\omega)} \quad \dots\dots\dots (2.11)$$

where $H(\omega)$ is amplitude function:

$$H(\omega) = \sum_{k=1}^M h(k)e^{-jk\omega} \quad \dots\dots\dots (2.12)$$

And $\theta(\omega)$ is phase function:

$$\theta(\omega) = \frac{M-1}{2} \omega \quad \dots\dots\dots (2.13)$$

2.3.2 Windowed Digital FIR Filter

If the desired frequency response $H_d(e^{j\omega})$ is defined, the inverse Fourier transform is usually used to calculate the filter coefficients:

$$h_d(n) = \frac{1}{2\pi} \int_{-\pi}^{\pi} H_d(e^{j\omega})e^{j\omega n} d\omega \quad \dots\dots\dots (2.14)$$

Generally $h_d(n)$ is an infinite sequence, and $h(n)$ is a finite sequence. Using these coefficients based on the inverse Fourier transform will only approximate the desired response because the number of filter coefficients is finite. Therefore, a window function may be applied to truncate the infinite filter coefficients. If a cutoff frequency ω_c is given, we have:

$$h(n) = \frac{1}{2\pi} \int_{-\pi}^{\pi} H_d(e^{j\theta})W(e^{j(\omega-\theta)})d\theta \quad \dots\dots\dots (2.15)$$

Where $W(e^{j\omega})$ is the frequency response window function $w(n)$:

$$W(e^{j\omega}) = \sum_{k=1}^M w(k)e^{-jk\omega} \quad \dots\dots\dots (2.16)$$

If Hamming window is used, the frequency response of FIR filter can be expressed:

$$H_w(e^{j\omega}) = H_w(\omega)e^{j\theta_w(\omega)} \quad \dots\dots\dots (2.17)$$

Where $H_w(\omega)$ is amplitude function:

$$H_w(\omega) = \frac{1}{2\pi} \int_{-\pi}^{\pi} H_d(\theta)W_R(\omega-\theta)d\theta \quad \dots\dots\dots (2.18)$$

Where $W_R(\omega)$ is the frequency response of Hamming window function.

2.3.3 Signal Decomposition

In power systems, the voltage and current signals always include high order harmonics, and in some cases the harmonics in these non-sinusoidal signals are also always not integral ones. In order to estimate the frequency of these non-integral harmonics, in this paper, we decompose the non-sinusoidal signals into different sinusoidal signals in different frequency scope using FIR filter based on Hamming window. Low-pass and band-pass filters are used to implement this aim.

The FIR filter coefficients, $h(k)$ ($k = 1, 2, M$), is different if the cutoff frequency in low-pass filters is set different value, and the filtering results are different. It is assumed that the harmonic frequencies are greater than 50Hz. For fundamental frequency, a low-pass FIR filter with a cutoff frequency of 60Hz is used. For high order harmonic frequency, band-pass FIR filters with a pass-band frequency of 60Hz are used. After sampling the non-sinusoidal signal with a sampling frequency of f_s , based on these sampling data sequences, we can decompose the non-sinusoidal signal into fundamental sinusoidal signal and other sinusoidal signals of non- integral harmonic.

A non-sinusoidal signal with K order non-integral harmonics has the following formula:

$$x(t) = V_1 \sin(2\pi f_1 + \phi_1) + V_2 \sin(2\pi f_2 + \phi_2) + \dots + V_K \sin(2\pi f_K + \phi_K) \quad \dots\dots\dots (2.19)$$

where $f_1 < f_2 < f_3 \dots < f_K$.

Using a low-pass FIR filter with a cutoff frequency f_c of 60Hz, the fundamental sinusoidal signals can be split out of the non-sinusoidal signal, and the output $y_1(n)$ of the low pass FIR filter in discrete time is written:

$$y_1(n) = \sum_{k=1}^M h_1(k)x(n-k) \quad \dots\dots\dots (2.20)$$

where $h_1(k)$ is the coefficients of the low-pass FIR filter for frequency band $[0,60]$, $x(n)$ is the sampling data sequence with a sampling frequency of f_s , $n = 1, 2, \dots, N$ where N is sampling number in a period of power system signals.

Filtering the non-sinusoidal signal using a pass-band frequency of a band-pass FIR filter with a lower cutoff frequency $f_{2,c,low}$ of 60Hz and a higher cutoff frequency $f_{2,c,high}$ of 120Hz, we can filter the sinusoidal signal out of non-sinusoidal signal in frequency band $[60,120]$:

$$y_2(n) = \sum_{k=1}^M h_2(k)x(n-k) \quad \dots\dots\dots (2.21)$$

where $y_2(n)$ is discrete value of the sinusoidal component in frequency band [60,120], $h_2(k)$ is the coefficients of the band-pass FIR filter for frequency band [60,120].

In the same way, a lower cutoff frequency $f_{i,c,low}$ of $60 \times i$ Hz and a higher cutoff frequency $f_{i,c,high}$ of $120 \times i$ Hz are set to a band-pass FIR filter, the discrete equation of the i^{th} sinusoidal component in frequency band [$60 \times i$, $120 \times i$] is obtained:

$$y_i(n) = \sum_{k=1}^M h_i(k)x(n-k) \dots\dots\dots (2.22)$$

where $h_i(k)$ is the coefficients of the band-pass FIR filter for frequency band [$60 \times i$, $120 \times i$], i is band-pass FIR filter number, $i = 2, \dots, I$, $I = \frac{f_s}{60}$. The sampling frequency f_s depends on the harmonic number K and f_s should be integer fold of 60.

After digital filtering of one time of low-pass FIR filter and digital filtering of I time of band-pass FIR filter, all sinusoidal components in the non-sinusoidal signal are filtered out.

2.3.4 Frequency Estimation of Sinusoidal Signals

A sinusoidal signal with a frequency of f is written as follow:

$$x(t) = V \sin(2\pi ft + \phi) \dots\dots\dots (2.23)$$

Where ϕ is the phase angle of the sinusoidal signal. After sampled with a sampling frequency of f_s , the discrete-time sequence of the sinusoidal signal can be rewritten:

$$x(n) = V \sin(2\pi f \frac{nT}{N} + \phi) = V \sin(2\pi ft_s + \phi) \dots\dots\dots (2.24)$$

where $t_s = \frac{nT}{N}$.

The 1st order differentiation of $x(n)$ with respect to t_s is:

$$x'(n) = 2\pi fV \cos(2\pi f \frac{nT}{N} + \phi) \dots\dots\dots (2.25)$$

The 2nd order differentiation is:

$$x''(n) = (2\pi f)^2 V \sin(2\pi f \frac{nT}{N} + \phi) \dots\dots\dots (2.26)$$

Based on numerical differentiation we can compute $x''(n)$ as:

$$x''(n) = \{2[x(p+3) + x(p-3)] - 27[x(p+2) + x(p-2)] + 270[x(p+1) + x(p-1)] - 490x(p)\} / 180h^2 \dots\dots\dots (2.27)$$

From (17), we have:

$$x''(n) = (2\pi f)^2 x(n) \dots\dots\dots (2.28)$$

Using (19), the frequency of the sinusoidal signal is estimated by:

$$f = \frac{1}{2\pi} \sqrt{\frac{-x''(n)}{x(n)}} \dots\dots\dots (2.29)$$

2.3.5 Harmonic Frequency Estimation

Using digital FIR filter, we can obtain the discrete value of each sinusoidal component of the non-sinusoidal signal with K order non-integral harmonics. The split sinusoidal component out of the non-sinusoidal signal may be expressed mathematically in continuous time:

$$x_i(t) = V_i \sin(2\pi f_i t + \phi_i) \dots\dots\dots (2.30)$$

Using the discrete value of each sinusoidal component of the non-sinusoidal signal, we can estimate the frequency of each sinusoidal component of the non-sinusoidal signal by respectively:

$$f_i = \frac{1}{2\pi} \sqrt{\frac{-y_i''(n)}{y_i(n)}} \dots\dots\dots (2.31)$$

2.4 IMPLEMENTATION

The algorithm proposed in this paper needs main steps for implementing harmonic frequency estimation of non-sinusoidal signals with high order harmonics. First, the non-sinusoidal signal is sampled to obtain the sampling data sequence. Second, digital low-pass and band-pass FIR filter are used to decompose the non-sinusoidal signal into individual sinusoidal component. Third, numerical differentiation is used to estimate the frequency of individual sinusoidal component of the non-sinusoidal signal. The detailed steps for algorithm implementation are written as follow:

- Step 1: Given band-pass FIR filter number, $i = 2, \dots, I$.
- Step 2: Given harmonic number, K .
- Step 3: Given sample number, N .
- Step 4: Given low-pass and band-pass FIR filter delay number, M .
- Step 5: Given the sampling frequency f_s according to the harmonic number.
- Step 6: Set the cutoff frequency $f_c = 60\text{Hz}$.
- Step 7: Set a lower cutoff frequency $f_{i,c,low}$ of $60 \times i$ Hz and a higher cutoff frequency $f_{i,c,high}$ of $120 \times i$ Hz for band-pass FIR filters, $i = 2, \dots, I$.
- Step 8: Compute $h_l(k)$ ($k=1 \dots M$) co-efficient of low pass FIR filter.
- Step 9: Compute $h_i(k)$ ($k=1, \dots, M$) ($i = 2, \dots, I$) coefficients of band-pass FIR filter.

Step 10: Sample the non-sinusoidal signal with a sampling frequency of $f_s=512*50$ Hz and obtain sampling data sequence $x(n)$.

Step 11: Compute the discrete output $y_1(n)$ of the low-pass FIR filter using equation (2.20).

Step 12: Compute the 2nd numerical differentiation $y_1''(n)$ of $y_1(n)$ using equation (2.27), setting $p=6$.

Step 13: Estimate the fundamental frequency f_1 of the non-sinusoidal signal using equation (2.31).

Step 14: set $i=2$.

Step 15: Compute the discrete output $y_i(n)$ of the band-pass FIR filter using equation (2.22).

Step 16: Compute the 2nd numerical differentiation $y_i''(n)$ of $y_i(n)$ using equation (2.27),

Step 17: Estimate the i^{th} order harmonic frequency f_i of the non-sinusoidal signal using equation (2.31).

Step 18: $i=i+1$.

Step 19: $i=I$? if No, then go to Step 14; if Yes, then end the algorithm work.

CHAPTER 3

SIMULATION RESULTS AND DISCUSSION

3.1 SIMULATION

Following test example, a voltage signal of 5 harmonic components was taken for computer simulation.

$$v(t) = V_1 \sin(2\pi f_1 + \phi_1) + V_2 \sin(2\pi f_2 + \phi_2) + V_3 \sin(2\pi f_3 + \phi_3) + V_4 \sin(2\pi f_4 + \phi_4) + V_5 \sin(2\pi f_5 + \phi_5) \dots\dots\dots (3.1)$$

where f_i , V_i and ϕ_i is the frequency, amplitude and phase angle of the i^{th} harmonic component respectively. f_i , V_i and ϕ_i is all unknown.

We assume that f_1 varies from 40Hz to 60Hz, f_2 varies from 200Hz to 300Hz, f_3 varies from 300Hz to 400Hz, f_4 varies from 500Hz to 600Hz, and f_5 varies from 700Hz to 800Hz. The fundamental amplitude varies from 0V to 300V, and other harmonic amplitude varies from 0V to 100V. The phase angle of all components varies from 0 to 360.

Various tests were carried out to test the sensitivity of the algorithm.

In any case, the signal is sampled with an initial sample frequency of 25600 Hz, and a sample sequence obtained from this sample is used for frequency estimation. The frequencies of the components 1, 2, 3, 4 and 5 of the signal are all estimated at an accuracy of 0.001% over 1 Hz to 800 kHz, as shown in Table I-Table V. The simulation is accomplished in 4 cases:

Case 1: the amplitude of the components 1, 2, 3, 4 and 5 of the signal are set to vary from 180 V to 260 V and 1 to 50 V at random respectively and the phase angle of the components 1, 2, 3, 4 and 5 of the signal are set to a fixed value, say $\phi_1=23^\circ$, $\phi_2=31^\circ$, $\phi_3=45^\circ$, $\phi_4=55^\circ$, $\phi_5=19^\circ$. The results of the simulation show that the accuracy for frequency estimation of the components are all 0.001% with the amplitude of the 1st, harmonic varying from 180 V to 260 V and 2nd, 3rd, 4th and 5th harmonic varying from 1 V to 50V respectively.

Case 2: the phase angle of the components 1, 2, 3, 4 and 5 of the signal is set to vary randomly from 0° to 360° respectively and the amplitude of the components of the signal are set to a fixed value, say $V_1=220$ V, $V_2=60$ V, $V_3=40$ V, $V_4=20$ V, $V_5=10$ V. In this case, the frequencies of the components of the signal are all estimated at an accuracy of 0.001% over 1 Hz to 800 kHz.

Case 3: the frequency of the sine noise is set to vary randomly from 0Hz to 300Hz respectively. The amplitude of the components of the signal are set to a fixed value, say $V_1=220$ V, $V_2=60$ V, $V_3=40$ V, $V_4=20$ V, $V_5=10$ V also the phase angle of the components 1, 2, 3, 4 and 5 of the signal are set to a fixed value, say $\phi_1=23^\circ$, $\phi_2=31^\circ$, $\phi_3=45^\circ$, $\phi_4=55^\circ$, $\phi_5=19^\circ$. In this case, the frequencies of the components of the signal are all estimated at an accuracy of 0.001% over 1 Hz to 800 kHz.

Case 4: the frequency of the signal is time varying in nature and is given by the expression

$$\omega(k) = 2\pi[50 + \sin(2\pi \cdot 1 \cdot t_k) + 0.5 \sin(2\pi \cdot 6 \cdot t_k)] \dots\dots\dots (3.2)$$

The amplitude of the components of the signal are set to a fixed value, say $V_1=220$ V, $V_2=60$ V, $V_3=40$ V, $V_4=20$ V, $V_5=10$ V also the phase angle of the components 1, 2, 3, 4 and 5 of the signal are set to a fixed value, say $\phi_1=23^\circ$, $\phi_2=31^\circ$, $\phi_3=45^\circ$, $\phi_4=55^\circ$, $\phi_5=19^\circ$. In this case, the frequencies of the components of the signal are all estimated at an accuracy of 0.001% over 1 Hz to 800 kHz.

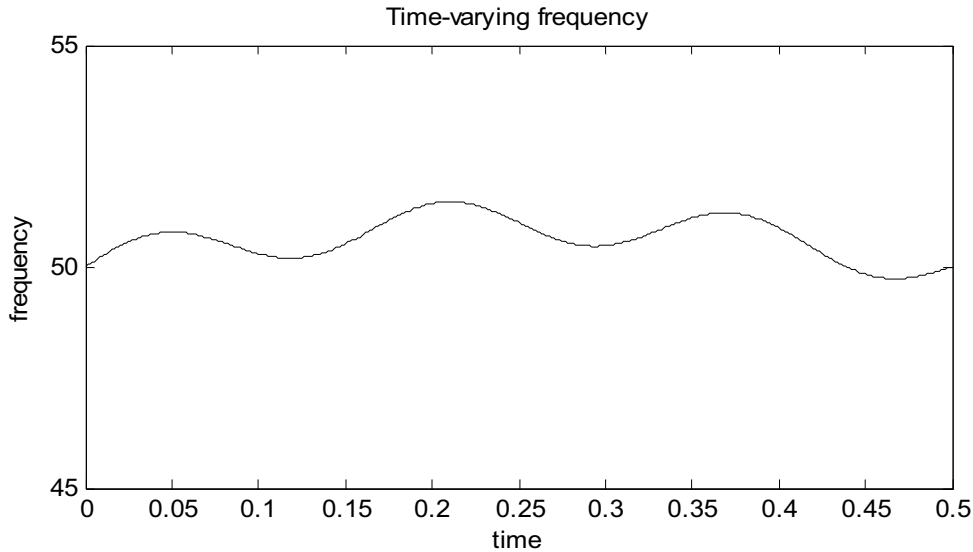


Figure 3.1

The tables' I-V shows the percentage of error in estimation of frequencies for a set of random data in case of 1st to 5th harmonics. The MATLAB simulation results for the cases stated above are shown in the form of plotted graphs in figures 3.2 -3.15.

Case 5: If the amplitude of the second to tenth order harmonics is much larger than the others, an equivalent harmonic is taken into consideration for replacing those high-order harmonics. Taking sixth-order harmonics for the central one, $x(n)$ and $x''(n)$ are replaced by

$$x(n) = V \sin(2\pi f \frac{nT}{N} + \phi_1) + \lambda V_6 \sin[\lambda(2\pi f) \frac{nT}{N} + \phi_6] \dots\dots\dots (3.3)$$

$$x''(n) = \sum_{k=1}^{10} [k2\pi f]^2 V_k \sin(2\pi kf \frac{nT}{N} + \phi_k) = -[k2\pi f]^2 V_1 \sin(2\pi kf \frac{nT}{N} + \phi_1) - \lambda [2\pi f \lambda]^2 V_6 \sin[\lambda(2\pi f) \frac{nT}{N} + \phi_6] \dots\dots\dots (3.4)$$

Where λ is a coefficient representing the influence of high-order harmonics. In mathematics, λ can be expressed as follows:

$$\lambda = \frac{2^2 \alpha_2 + 3^2 \alpha_3 + 4^2 \alpha_4 + 5^2 \alpha_5 + 6^2 \alpha_6 + 7^2 \alpha_7}{6^2 \alpha_2} + \frac{8^2 \alpha_8 + 9^2 \alpha_9 + 10^2 \alpha_{10}}{6^2 \alpha_2} \dots\dots\dots (3.5)$$

$\alpha_i (i=2, 3, 4, \dots, 10.)$ is the general proportion of i^{th} harmonic in the total magnitude of the sampled voltage signal. If fundamental signal is expressed as

$$x_1(n) = V_1 \sin(2\pi f \frac{nT}{N} + \phi_1) \dots\dots\dots (3.6)$$

Then $x''(n)$ is written as

$$\begin{aligned} x''(n) &= -\lambda^2 [2\pi f]^2 \{V_1 \sin(2\pi f \frac{nT}{N} + \phi_1) + \lambda V_6 [\sin \lambda(2\pi f) \frac{nT}{N} + \phi_6]\} + (\lambda^2 - 1) [2\pi f]^2 V_1 \sin(2\pi f \frac{nT}{N} + \phi_1) \\ &= -\lambda^2 [2\pi f]^2 x(n) + (\lambda^2 - 1) [2\pi f]^2 x_1(n) \dots\dots\dots (3.7) \end{aligned}$$

From (3.7), we obtain

$$x_1(n) = \frac{x''(n)}{(\lambda^2 - 1) [2\pi f]^2} + \frac{\lambda^2 x(n)}{(\lambda^2 - 1)} \dots\dots\dots (3.8)$$

From (3.8), we get

$$x_1''(n) = \frac{x^{(4)}(n)}{(\lambda^2 - 1) [2\pi f]^2} + \frac{\lambda^2 x''(n)}{(\lambda^2 - 1)} \dots\dots\dots (3.9)$$

From (3.9),

$$\begin{aligned} x_1''(n) &= x_1(n) [2\pi f]^2 \\ &= \left[\frac{x''(n)}{(\lambda^2 - 1) [2\pi f]^2} + \frac{\lambda^2 x(n)}{(\lambda^2 - 1)} \right] [2\pi f]^2 \dots\dots\dots (3.10) \end{aligned}$$

From (3.9) and (3.10),

$$\lambda^2 [2\pi f]^4 x(n) + (\lambda^2 + 1) [2\pi f]^2 x''(n) + x^{(4)}(n) = 0 \dots\dots\dots (3.11)$$

The frequency estimation sensitivity for different values of λ was tested. The simulated result is shown in figure 3.16.

3.2 RESULTS

Table-I

Frequency estimation of 1st harmonic of non-sinusoidal signals

No.	Real (Hz)	Estimated (Hz)	Error (%)
1	43.798	45.663	-0.0075
2	56.808	56.827	0.0193
3	52	52.036	0.0356
4	55.678	55.688	0.0103
5	50.503	50.544	0.0410
6	52.462	52.504	0.0423
7	57.62	57.636	0.0159
8	59.405	59.426	0.0213

Table-II

Frequency estimation of 2nd harmonic of non-sinusoidal signals

No.	Real (Hz)	Estimated (Hz)	Error (%)
1	236.76	236.6125	-0.1475
2	271.763	271.2587	-0.5043
3	207.80	206.9081	-0.8919
4	245.34	245.3496	0.0096
5	235.325	235.1612	-0.1638
6	218.25	217.8344	-0.4156
7	248.76	248.9688	0.2088
8	245	244.9984	-0.0016

Table-III

Frequency estimation of 3rd harmonic of non-sinusoidal signals

No.	Real (Hz)	Estimated (Hz)	Error (%)
1	314.345	314.4110	0.0660
2	316.585	316.6081	0.0231
3	327.502	327.2372	-0.2648
4	366.76	367.1034	0.3484
5	357.61	357.6790	0.0740
6	386.75	387.4273	0.6773
7	389.03	389.9020	0.8700
8	381.59	382.0215	0.4285

Table-IVFrequency estimation of 4th harmonic of non-sinusoidal signals

No.	Real (Hz)	Estimated (Hz)	Error (%)
1	532.89	533.2344	0.3444
2	512.68	511.9830	-0.6960
3	544.07	544.3181	0.2491
4	503.49	503.1755	-0.3135
5	539.72	539.9844	0.2664
6	565.52	565.9475	0.4265
7	523	523.8164	0.8164
8	598	597.4201	-0.5799

Table-VFrequency estimation of 5th harmonic of non-sinusoidal signals

No.	Real (Hz)	Estimated (Hz)	Error (%)
1	741.03	740.0745	-0.9595
2	756.39	755.7652	-0.6248
3	768.92	768.1412	-0.7788
4	772.09	771.1883	-0.9037
5	735.09	735.9631	0.8711
6	739.54	740.1550	0.6150
7	719.14	718.3419	-0.7981
8	705.04	704.7399	-0.3001

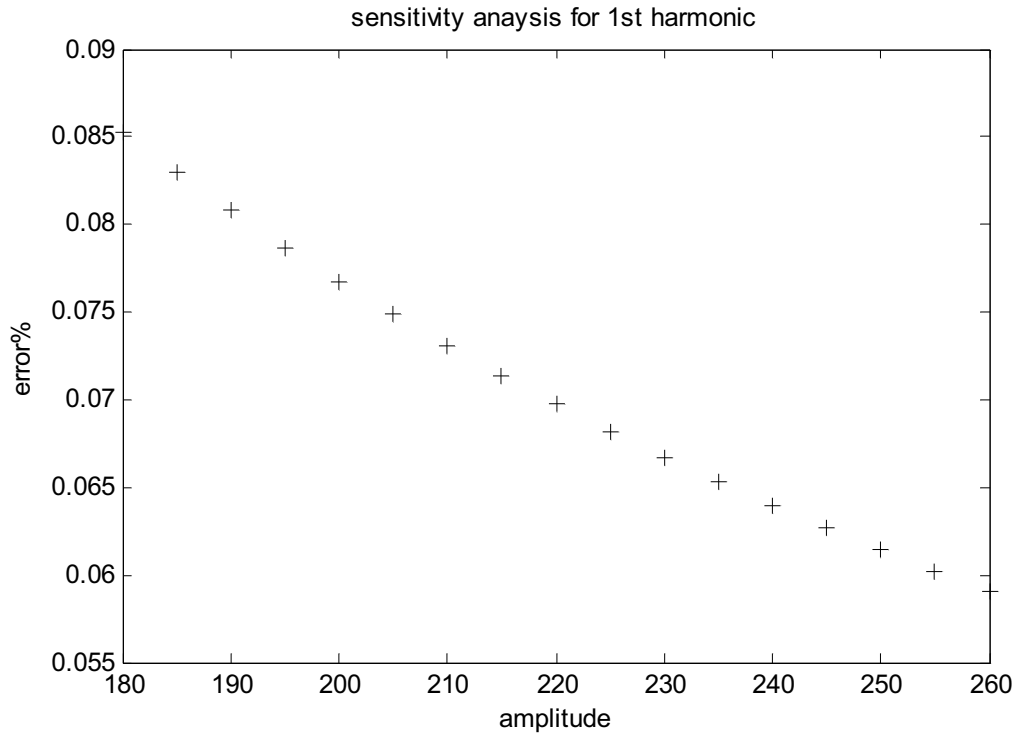


Figure 3.2

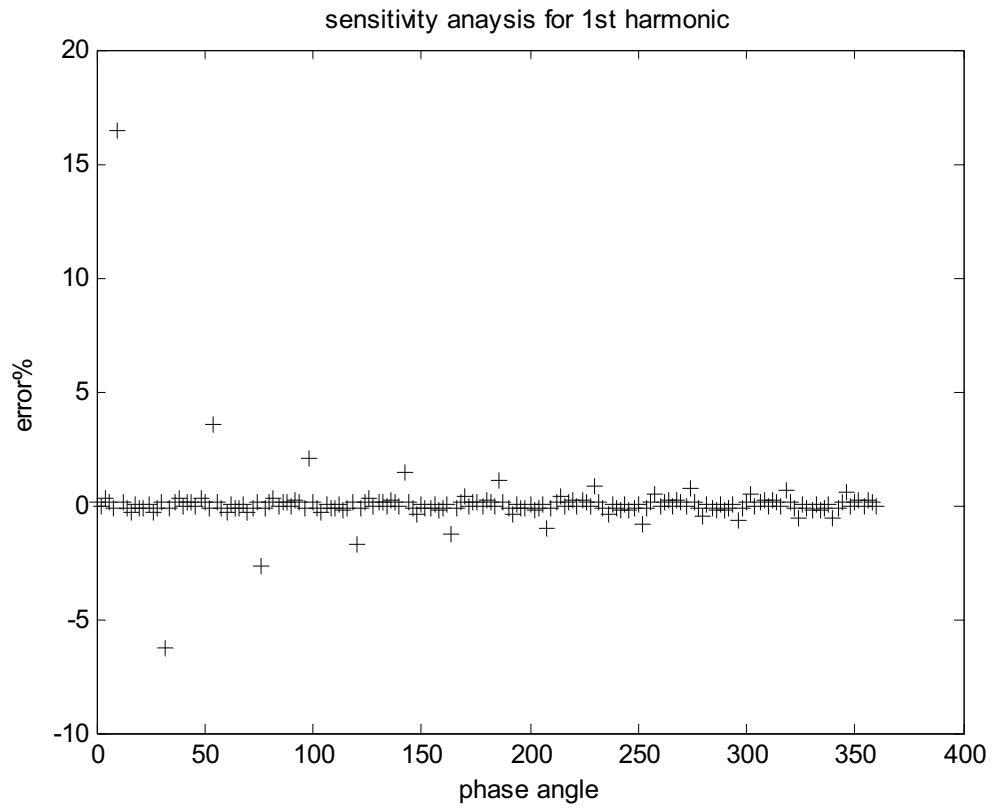


Figure 3.3

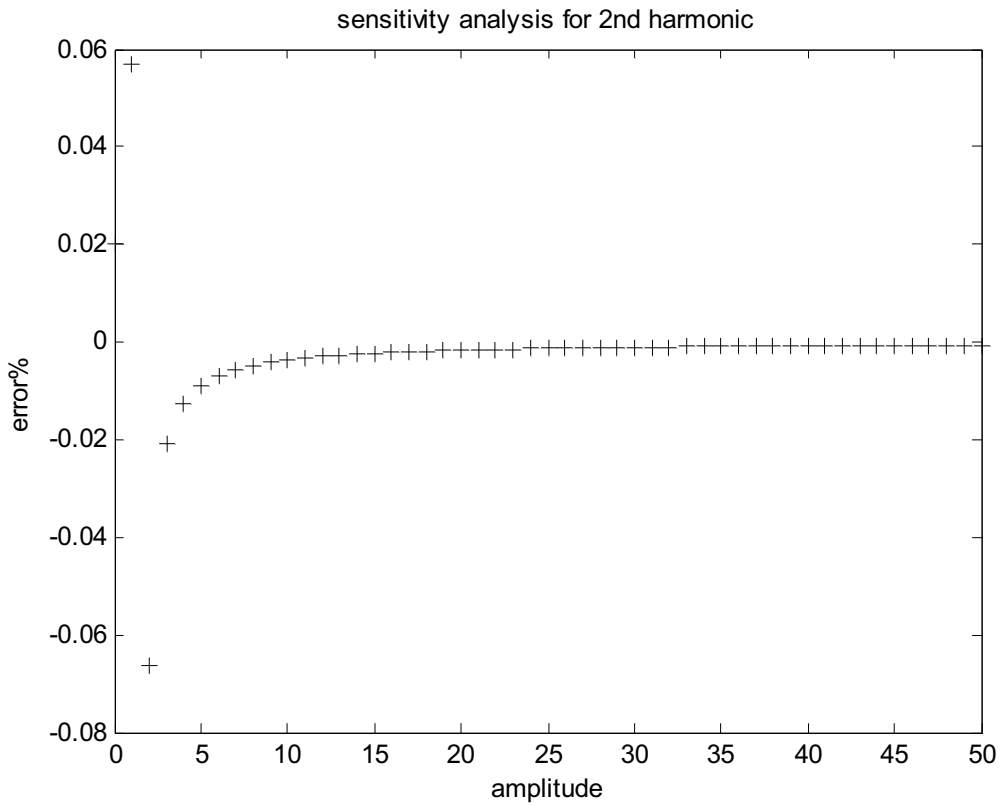


Figure 3.4

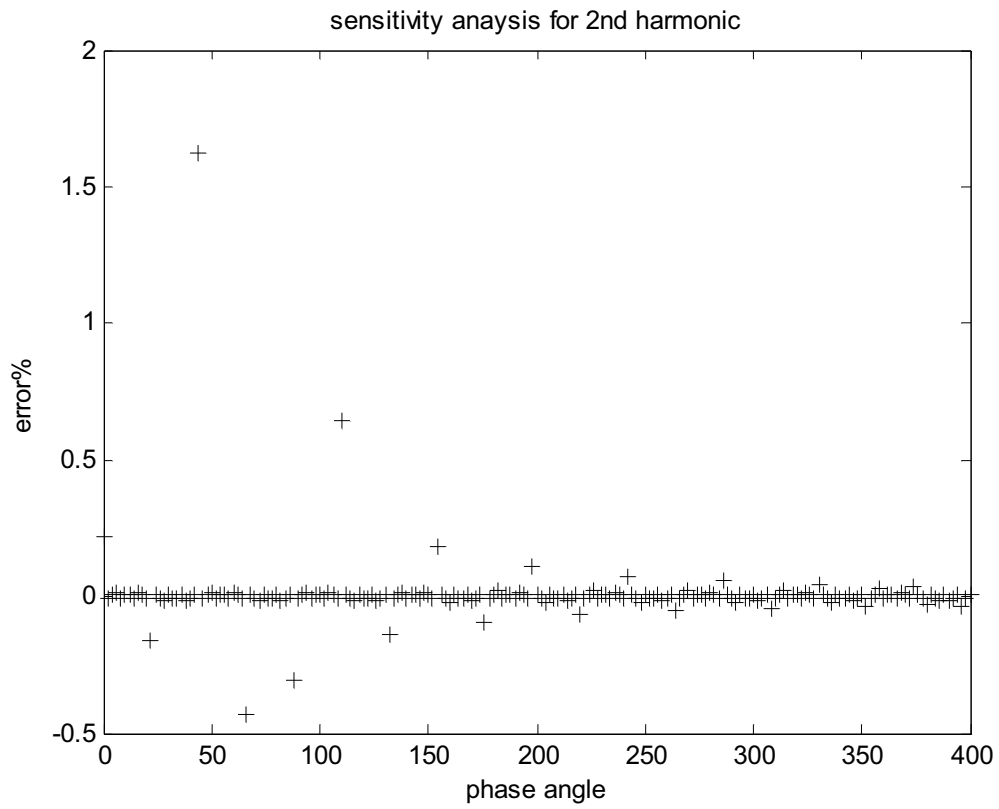


Figure 3.5

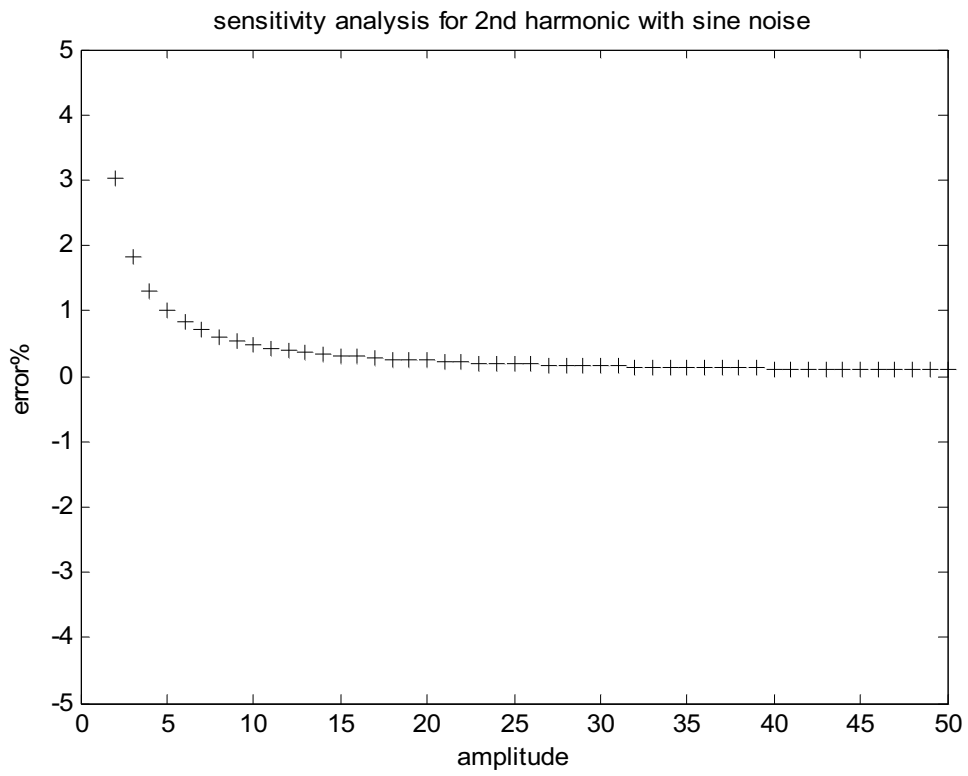


Figure 3.6

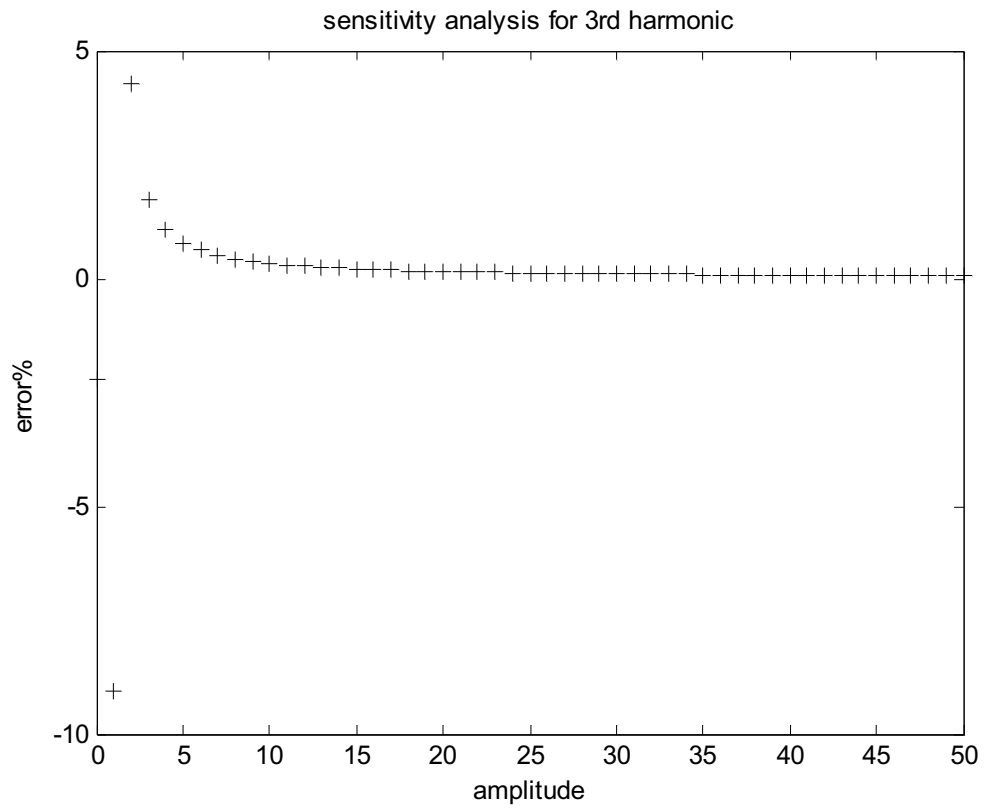


Figure 3.7

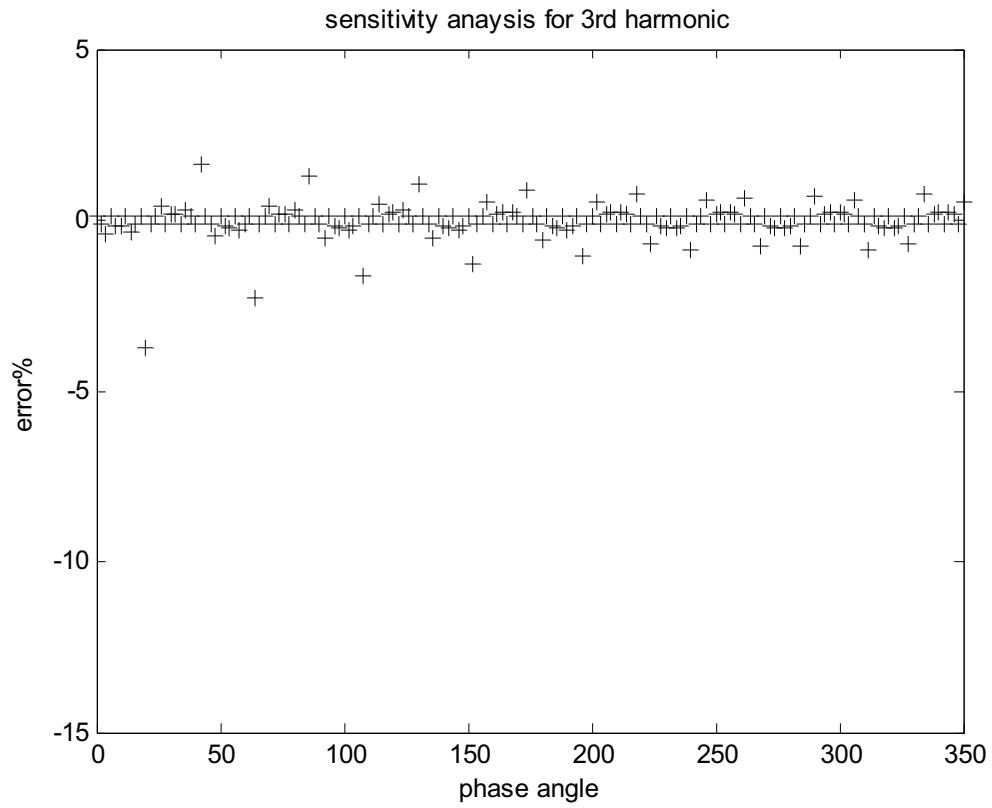


Figure 3.8

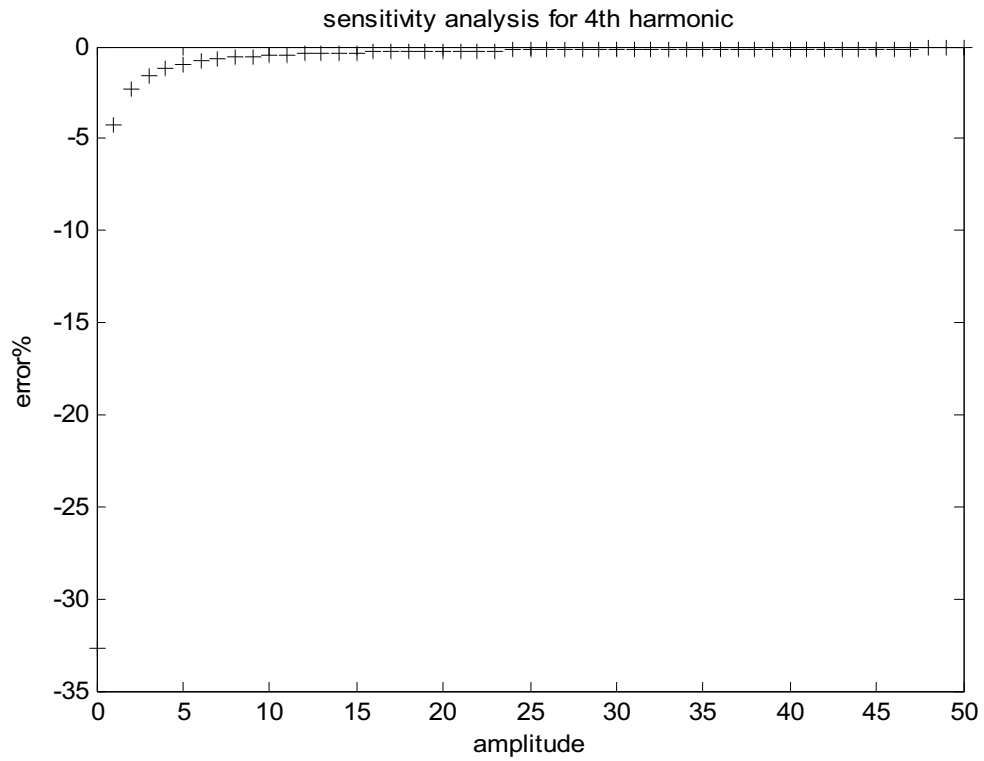


Figure 3.9

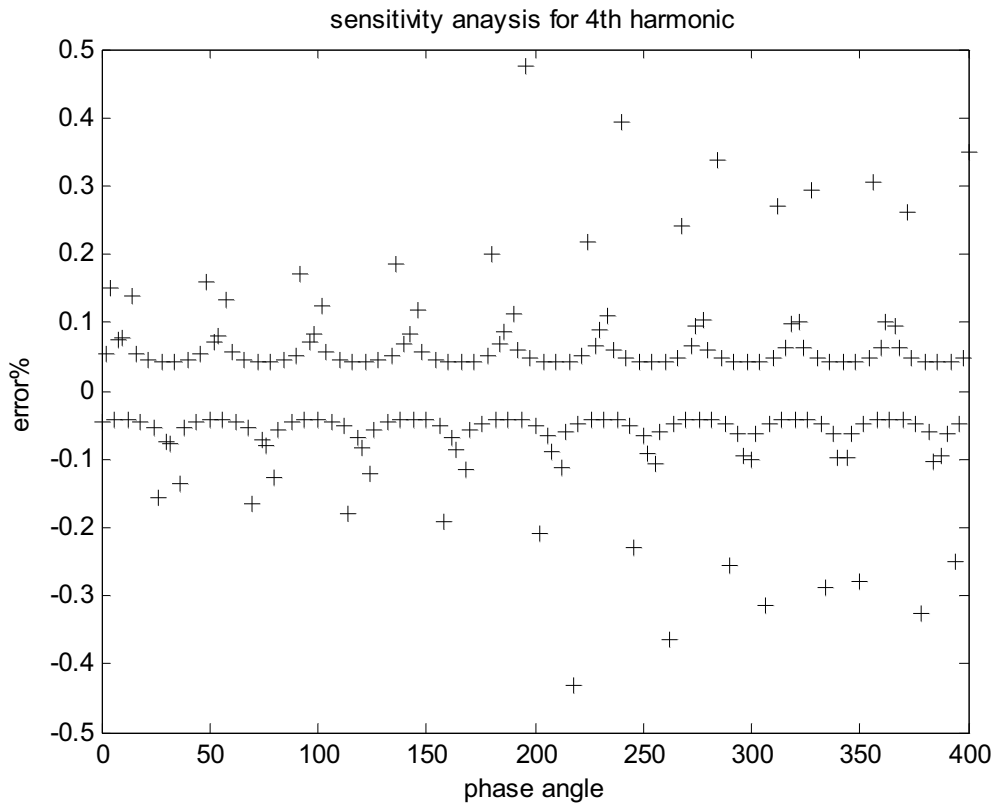


Figure 3.10

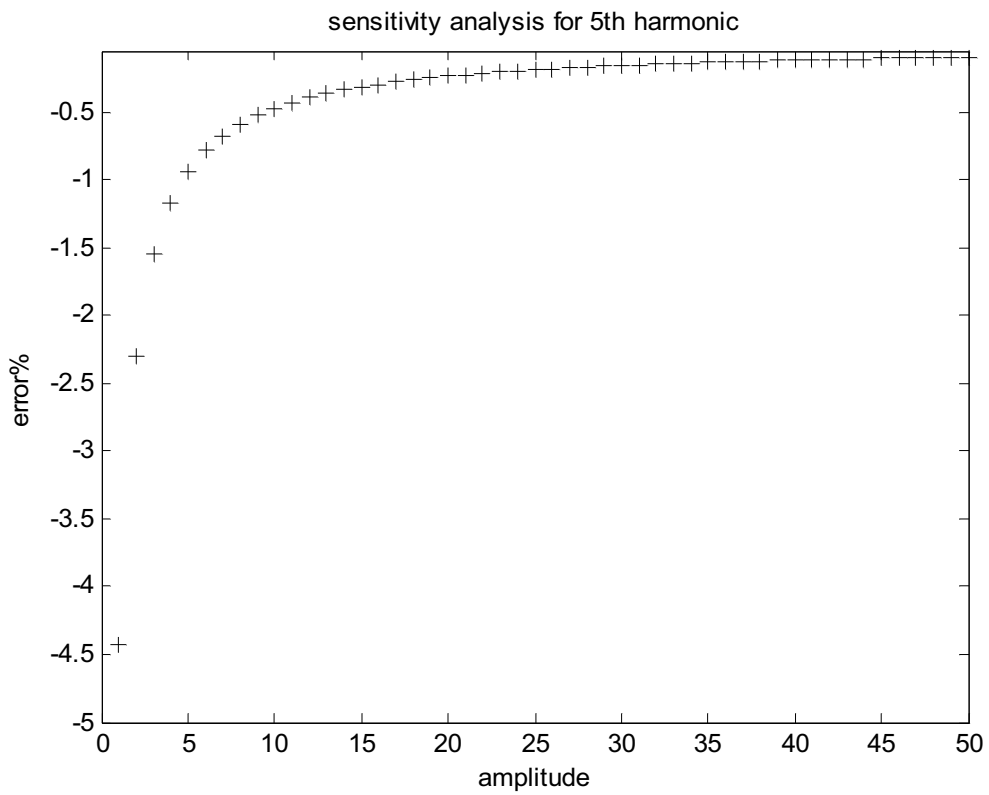


Figure 3.11

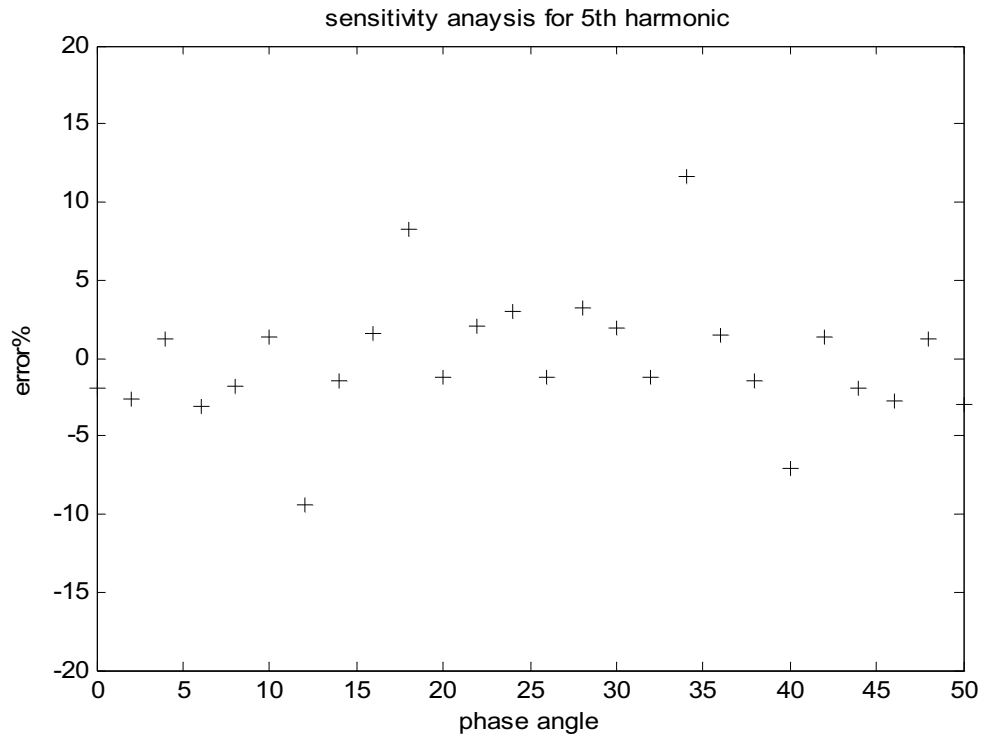


Figure 3.12

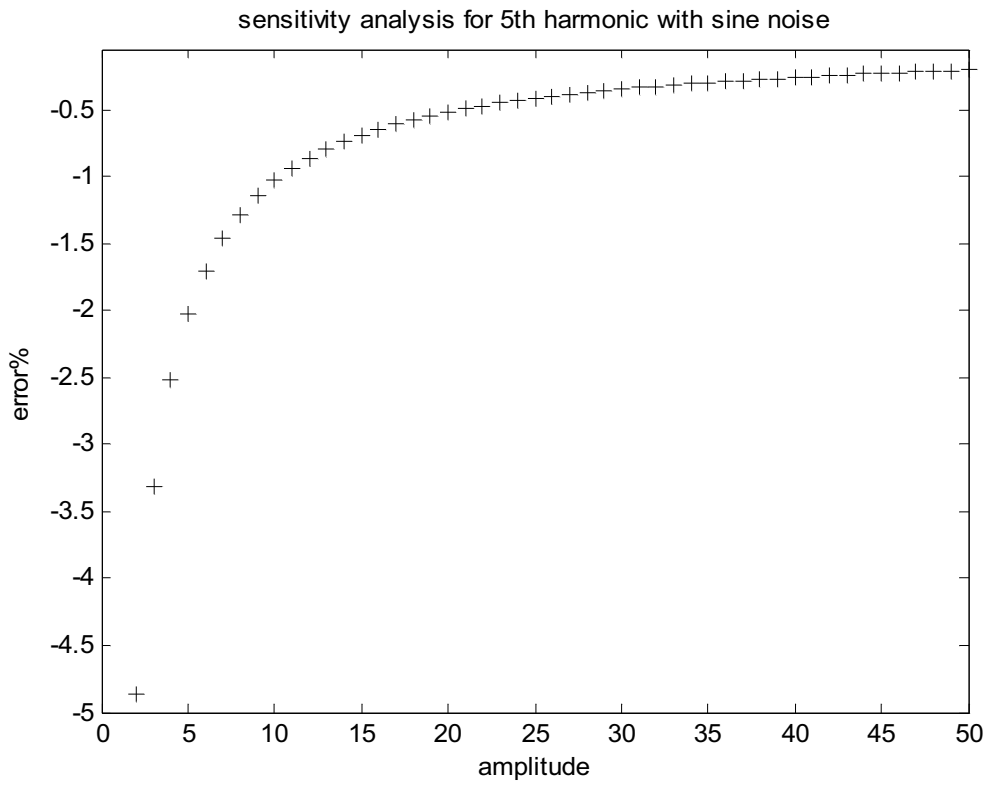


Figure 3.13

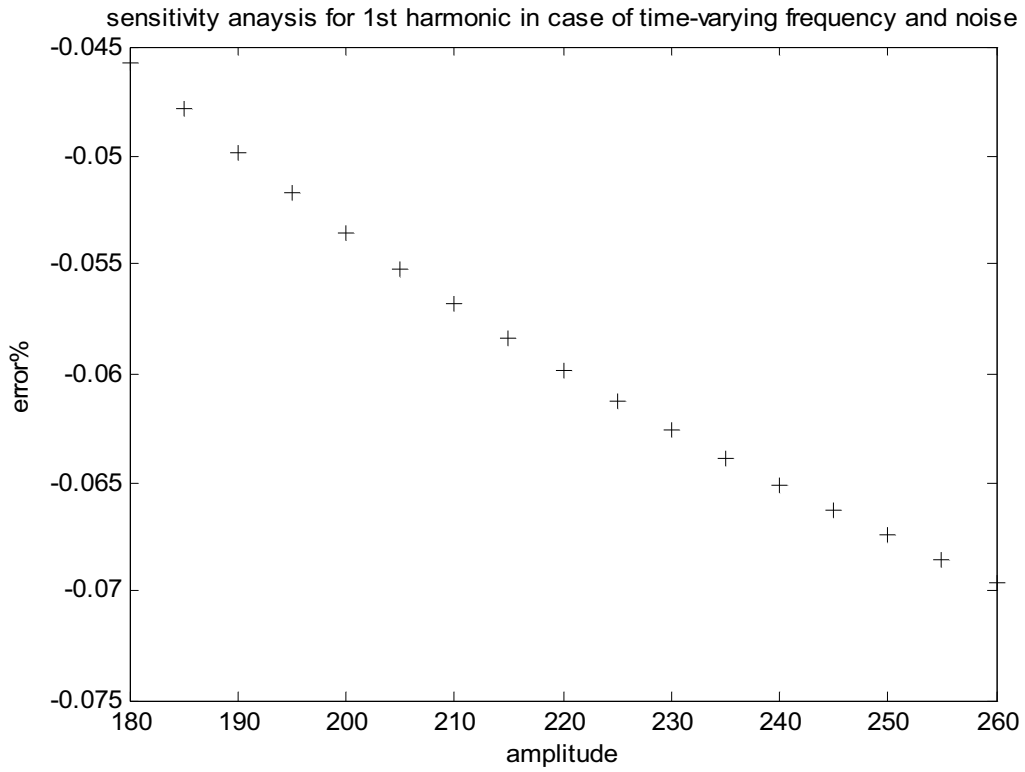


Figure 3.14

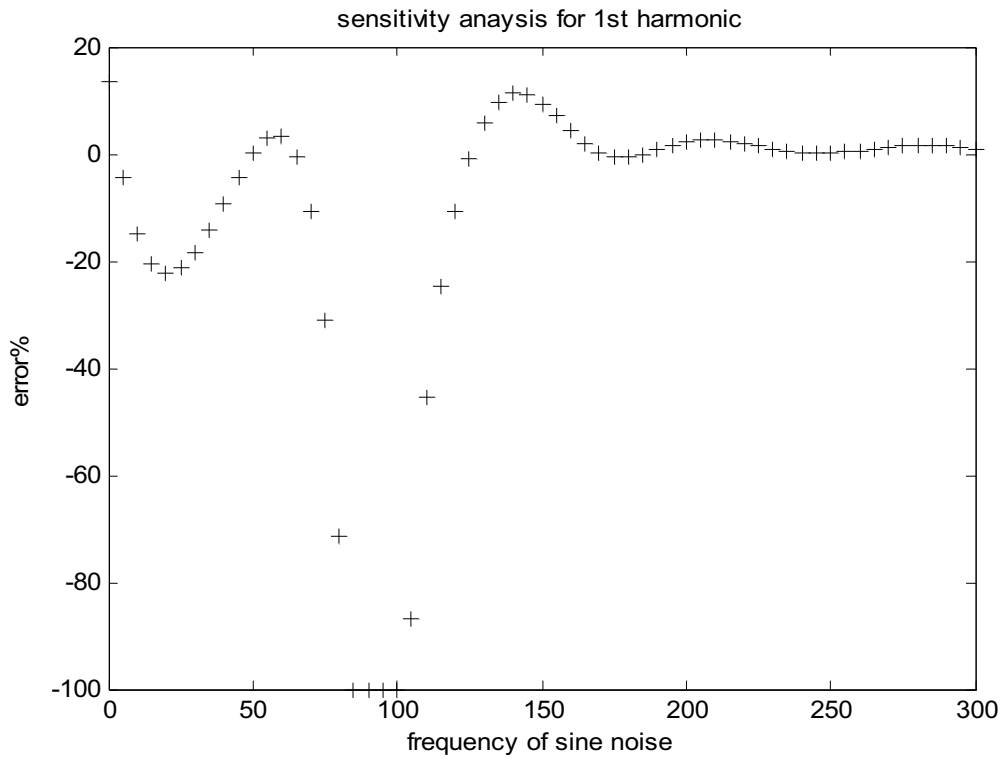


Figure 3.15

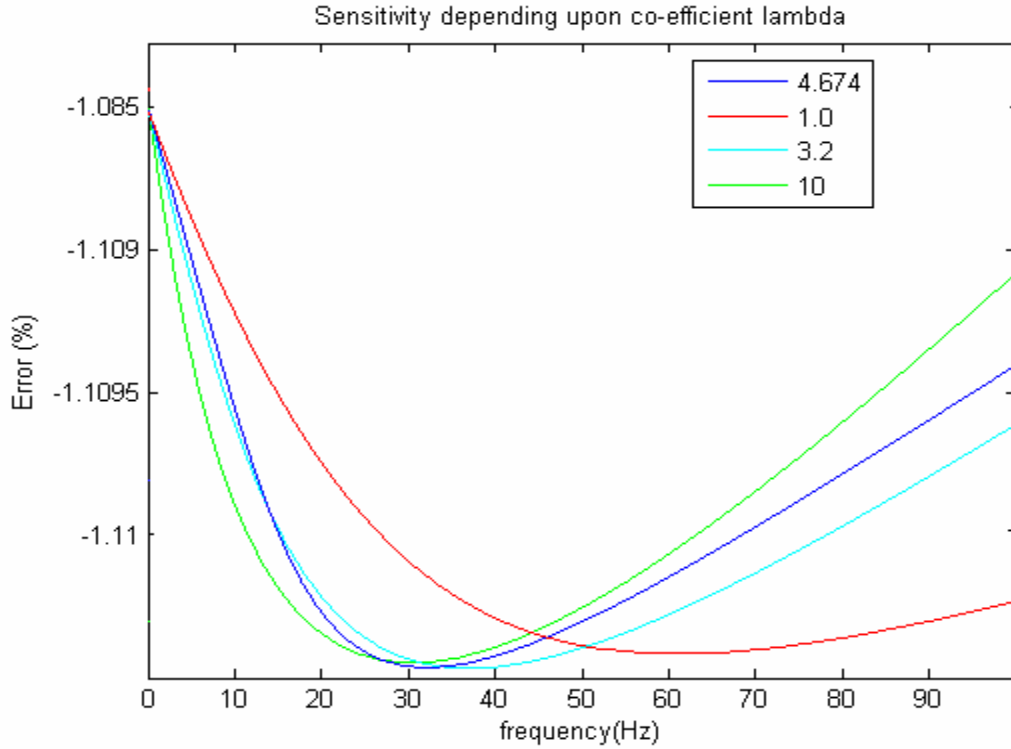


Figure 3.16

3.3 DISCUSSION

Table I shows the dynamic characteristic of the proposed algorithm for the fundamental frequency estimation. From the data of Table I, the estimation error is at most 0.04% when its value varies from 40Hz to 60Hz. Fig.3.2 and Fig.3.3 show the sensitivity analysis of the fundamental frequency estimation for the amplitude and phase angle of the 1st harmonic. The amplitude varying from 180V to 260V.

Table II shows the dynamic characteristic of the proposed algorithm for the 2nd harmonic frequency estimation and Fig.3.4 and Fig.3.5 shows the sensitivity analysis of the 2nd harmonic frequency estimation for the amplitude and phase angle of the 2nd component of the non-sinusoidal signal respectively. From the data of Table II, the estimation error is at most 0.8 % when its value varies from 200Hz to 300Hz. With the amplitude of the 2nd component of the non-sinusoidal signal varying from 0V to 50V, the estimation error increases from -0.8% to 0.2%. Figure 3.6 shows the estimation error of 2nd harmonic with the amplitude in case of sine noise. The graph converges to 0.

Table III shows the dynamic characteristic of the considered algorithm for the 3rd harmonic frequency estimation and Fig.3.7 and Fig.3.8 shows the sensitivity analysis of the 3rd harmonic frequency estimation for the amplitude and phase angle of the 3rd component of the non-sinusoidal signal respectively. From the data of Table III, the estimation error is at most 0.8% when its value varies from 300Hz to 400Hz. With the amplitude of the 3rd component of the non-sinusoidal signal varying from 0V to 50V, the estimation error increases from -6% to 0.

Table IV shows the dynamic characteristic of the considered algorithm for the 4th harmonic frequency estimation and Fig. 3.9 and Fig.3.10 shows the sensitivity analysis of the 4th harmonic frequency estimation for the amplitude and phase angle of the 4th component of the non-sinusoidal signal respectively. From the data of Table IV, the estimation error is at most 0.8% when its value varies from 500Hz to 600Hz. With the amplitude of the 4th component of the non-sinusoidal signal varying from 0V to 50V, the estimation error increases from 5 % to 0.

Table V shows the dynamic characteristic of the considered algorithm for the 5th harmonic frequency estimation and Fig.3.11 and Fig.3.12 shows the sensitivity analysis of the 5th harmonic frequency estimation for the amplitude and phase angle of the 5th component of the non-sinusoidal signal respectively. From the data of Table V, the estimation error is at most 0.8% when its value varies from 700Hz to 800Hz. With the amplitude of the 5th component of the non-sinusoidal signal varying from 0V to 50V, the estimation error increases from -0.6% to -0.02%.

Fig. 3.15 shows the sensitivity of frequency estimation of power systems for the frequency change of sine noises. The error varies between 0 to $-\infty$ either increasing or decreasing, when the frequency of sine noises change from 0-70 Hz. Between 70Hz – 300 Hz, the errors first increase from $-\infty$ to 0, further increasing and then settling down nearly to 0.

In the Table-VI shown overleaf, the estimation error of NDF(Numerical differentiation and FIR algorithm) are compared to other techniques, such as DFT(Discrete Fourier Transform), and EFFT(Enhanced Fast Fourier Transform).The data of DFT is obtained from [20] and that of EFFT is obtained from[17].

TABLE-VI

True	NDF	DFT	E-FFT
50.0	49.992	49.99	49.99
86.6	86.5674	86.64	86.59
150.0	149.944	149.96	150.0

CHAPTER 4

CONCLUSION

4.1 CONCLUSION

The methodology to the considered algorithm for harmonic frequency estimation is to decompose the non-sinusoidal signal with high order harmonics into different individual sinusoidal components and then estimate the frequency of each decomposed sinusoidal signal using numerical differentiation. Numerical differentiation algorithm is characteristic of high accuracy and much less time. For a non-sinusoidal signal of 5 order harmonics, at most one and a half cycle, in the first estimation process, and requires at most half cycle, in the latter estimation. Some existing techniques always employ such algorithms as FFT (Fast Fourier Transform), DFT (Discrete Fourier Transform) and Prony's method to estimate the frequency and speed much computation time.

4.2 SCOPE OF FUTURE WORK

Improvement can be brought about in the design of the digital FIR filter used in the proposed method. When the harmonic frequencies in the non-sinusoidal signal are in closely spaced range, the determination of the cut-off frequencies of the band-pass filter used, becomes a major problem. Thus, it becomes a disadvantage. The algorithm considered uses a Hamming window. Further work can be done by using other windowing methods such as Hanning window, Rectangular window, and etcetera.

REFERENCES

- [1] M. M. Begovic, P. M. Djuric, S. Dunlap and A. G. Phadke, "Frequency tracking in power networks in the presence of harmonics," IEEE Trans. On Power Delivery, April, 1993, Vol.8, No.2, pp.480–486.
- [2] A. K. Hacaoğlu and M. J. Devaney, "A new quadratic form based frequency measurement algorithm," in IEEE Instr. and Meas. Tech. Conference, Brussels, Belgium, June 4–6, 1996, pp. 1065–1070.
- [3] M. S. Sachdev and M. M. Giray, "A least error squares technique for determining power system frequency," IEEE Trans. on Power Apparatus and Systems, Feb., 1985 Vol.104, No.2, pp.437–443.
- [4] M. M. Giray and M. S. Sachdev, "Off-nominal frequency measurements in electric power systems," IEEE Trans. on Power Delivery, July, 1989, Vol.4, No.3, pp.1573–1578.
- [5] V. V. Terzija, M. B. Djuric and Kovacevic B D, "Voltage phasor and local system frequency estimation using Newton type algorithm," IEEE Trans. On Power Delivery, , July, 1994, Vol.9, No.3, pp.1368–1374.
- [6] M. S. Sachdev, H. C. Wood and N. G. Johnson, "Kalman filtering applied to power system measurements for relaying," IEEE Trans. On Power Apparatus and System, , Dec., 1985, Vol.104, No.12, pp.3565–3573.
- [7] A. A. Girgis and T. L. D.Hwang, "Optimal estimation of voltage phasors and frequency deviation using linear and nonlinear kalman filter: Theory and limitations," IEEE Trans. on Power Apparatus and Systems, Vol.103, No.10, pp.2943–2949.
- [8] A. A. Girgis and W. L. Peterson, "Adaptive estimation of power system frequency deviation and its rate of change for calculating sudden power system overloads," IEEE Trans. on Power Delivery, , Apr., 1990, Vol.5, No.2, pp.585– 594.
- [9] T. Lobos and J. Rezmer, "Real time determination of power system frequency," IEEE Trans. on Instrumentation and Measurement, Aug., 1997, Vol.46, No.4, pp.877–881.

- [10] A. G. Phadke, J. S. Thorp and M. G. Adamiak, "A new measurement technique for tracking voltage phasors, local system frequency, and rate of change of frequency," IEEE Trans. on Power Apparatus and Systems, May, 1983, Vol.102, No.5, pp.1025–1038.
- [11] J. Z. Yang and C. W. Liu, "A Precise Calculation of Power System Frequency," IEEE TRANSACTIONS ON POWER DELIVERY, July, 2001, Vol.16, No.3, pp.361-366,.
- [12] J. Z. Yang and C. W. Liu, "A Precise Calculation of Power System Frequency and Phasor," IEEE TRANSACTIONS ON POWER DELIVERY, Apr., 2000 Vol.15, No.2, pp.494-499.
- [13] S. L. Lu, C. E. Lin and C. L. Huang, "Power frequency harmonic measurement using integer periodic extension method," Electric Power systems Research, Vol.44, No.2, pp.107-115,.
- [14] P. J. Moore and A. T. Johns, "A new numeric technique for high-speed evaluation of power system frequency," IEE Pro.-Gener. Transm. Distrib, Sep., 1994, Vol.141, No.5, pp.529-536.
- [15] J. Szafran and W. Rebizant, "Power system frequency estimation," IEE Pro.-Gener. Transm. Distrib, Sep., 1998, Vol.145, No.5, pp.578-582.
- [16] A. A. Girgis and F. M. Ham, "A new FFT-based digital frequency relay for load shedding," IEEE Transactions on Power Apparatus and Systems, Feb., 1982, Vol.101, pp.433-439,.
- [17] H. C. Lin and C. S. Lee, "Enhanced FFT-based parameter algorithm for simultaneous multiple harmonics analysis," IEE Pro.-Gener. Transm. Distrib, May, 2001, Vol.148, No.3, pp.209-214.
- [18] M. Akke, "Frequency estimation method by demodulation of complex signals," IEEE Trans. on Power Delivery, , Jan. 1997, vol. 12, pp. 157–163.
- [19] M. El-Shafey, "Beating the Nyquist limit by utilizing samples of filtered sinusoids," in Proc. Int. Conf. Elect., Electron., Comp. Eng. Cairo, Egypt, 2004, pp. 210–213.

[20] V. L. Phvm and K. P. Wang. "Wavelet-transform-based algorithm for harmonic analysis of power system waveforms," IEE Proceedings-Generation, Transmission, Distribution, Vol.146, No.3, pp. 249 - 254.

[21] J. K. Wu, J. Long and J. X. Wang, "Harmonic Estimation in A Power System Basing on Numerical Differentiation," in the of Proceedings of the Fifth International Conference on Power Electronics and Drive Systems, Singapore, Singapore, Nov, 2003, pp.1574-1579

[22] P.J. Moore, R.D. Carranza and A.T. Johns, "A new numeric technique for high-speed evaluation of power system frequency", *IEE Proceedings-Generation Transmission and Distribution* **141** (1994) (5), pp. 529–536.